UCLouvain

École polytechnique de Louvain

Complexity and Quantization trade-offs for mm-Wave communication systems

Author: **Nicolas DE HALLEUX**
Supervisors: **Dr. Claude DESSET, Prof. Jérôme LOUVEAUX**
Reader: **Prof. Luc VANDENDORPE**
Academic year 2022–2023
Master [120] in Electrical Engineering

ACKNOWLEDGEMENTS

First and foremost, I would like to thank my supervisors Claude Desset and Jérôme Louveaux. This master's thesis would not have been possible without them. They were both always available to have a discussion about my research, to answer my questions, or to provide guidance on the way forward.

I would also like to thank Jérôme for giving me the opportunity and the contact to do an internship at IMEC and Claude for introducing me there. It has been a wonderful semester working there with a great team.

Thank you as well to Luc Vandendorpe for accepting to read my work and to Yiğit Ertuğrul and Martin Willame for reviewing my thesis.

Finally, I would like to thank all the persons who have encouraged and supported me, and who have contributed, whether directly or indirectly, to this thesis.

ABSTRACT

To provide an increasing volume of data rapidly via telecommunication devices, throughputs must be increased. With the new coming 5G and 6G, mm-Wave frequency designs are studied to be used because of their wider available frequency bands. In the context of sustainability, research on how to provide these throughputs with the least power consumed is needed. This thesis aims to optimize the digital baseband computation of mm-Wave communication systems for several scenarios in SISO and MU-MIMO. To estimate the power consumed, the number of digital operations is counted and is related to the quantization level. The optimal levels for each block of the digital part of the communication are analyzed. With this model, we show that for the optimal configuration around 20% of savings can be made compared to a full 10-bits computation.

CONTENTS

NOTATIONS

Accronymes

1G, . . .,6G	First to sixth Generation
ADC	Analog-to-Digital Converter
AGC	Automatic Gain Control
AWGN	Additive White Gaussian Noise
BER	Bit Error Rate
BF	Beamforming
BPSK	Binary Phase-Shift Keying
BW	Bandwidth
CE	Channel Estimation
CFO	Carrier Frequency Offset
CIR	Channel Impulse Response
CP	Cyclic Prefix
DAC	Digital-to-Analog Converter
DFT	Discrete Fourier Transform
DSP	Digital Signal Processing
EE	Energy Efficiency
FDM	Frequency Division Multiplexing
FFT	Fast Fourier Transform
LDPC	Low-Density Parity Check
LLR	Log Likelihood Ratio
LNA	Low Noise Amplifier
LoS	Line-of-Sight
LUT	Look-Up Table
MCT	Maximum Combining Transmission
MIMO	Multi Input Multi Output
MMSE	Minimum Mean Square Error
mm-Wave	Millimeter-Wave

MU-MIMO	Multi-User MIMO
NLoS	Non Line-of-Sight
OFDM	Orthogonal Frequency Division Multiplexing
PA	Power Amplifier
P/S	Parallel to Serial
QAM	Quadrature Amplitude modulation
RF	Radio Frequency
RX	Receiver
SCO	Sampling Clock Offset
SINR	Signal-to-Interference-plus-Noise Ratio
SIR	Signal-to-Interference Ratio
SISO	Single Input Single Output
SNR	Signal-to-Noise Ratio
SRRC	Square-Root Raised Cosine
S/P	Serial to Parallel
TX	Transmitter
ZF	Zero-Forcing

1 INTRODUCTION

1.1 Context

In a context where telecommunication and data are widely used, the need for more sustainable and efficient communication becomes more and more important. Additionally, with the ever-increasing throughputs, new systems for mm-Wave will have to adopt other schemes such as wider bandwidth, Multiple Input Multiple Output (MIMO) techniques and/or spatial diversity, etc [14]. As fifth-generation (5G) systems begin to take place, the research for 6G is already undergoing. 6G would enable terabit-per-second data rates and would allow the Internet of Things to become a reality. But at these frequencies, the power consumption will become a challenge[35].

Telecommunications chains are made of an analog part comprehending the antennas, beamforming networks, amplifiers, and local oscillators and the digital part with all the processing of the data to be sent/received. For the analog part at the transmission for example, at the base station 75% of the power is consumed in the Power Amplifier (PA) [1]. Working for wider bandwidths means also working with a higher sampling frequency for the digital signal processing part (DSP) which lead to a higher power consumption.

The trade-off between power consumption and performance is a fundamental challenge in telecommunication systems design. Finding the optimal balance between power consumption and performance is crucial to achieve efficient and sustainable communication systems. Therefore, understanding the relationship between power consumption and performance is essential in developing energy-efficient telecommunication solutions.

The used scheme is multi-user MIMO (MU-MIMO) with Hybrid beamforming however single input single output (SISO) will also be taken into consideration at the start of this research.

A lot of papers characterize the power of a specific telecommunication chain and it is usually done with hardware measurements [34] [5] [42]. They perform one type of communication, optimize one design, and then show the power consumption.

A model to quantify the power consumption of the entire wireless system was created at IMEC, the Base Station power model. The model was taking the power estimates of the PAs, the BaseBand (BB) unit, the power supply and cooling systems, etc to see the impact of the traffic on the network. It revealed that for older generations, the power consumed by the network was not dependent on the traffic of data load [4]. The model then evolved with the new generation to be more flexible on the scenario used, to have a model for many types of architectures [10]. This power model has for goal to be able to estimate the global power consumption that each design could have. This approach gives for each scenario, the power consumption in a theoretical way, before the hardware implementation of the chain. The model used is very versatile and makes it possible to compare the power consumption of several scenarios. This would allow us to analyze more thoroughly the optimal scheme for a specific application with regard to the type of coding rate, modulation, filter size, multiple streams, bandwidth, etc. This way, we can analyze which type of communication system would be best to create to have the most energy-efficient design. This model comes from a previous paper of IMEC [10]. A part of this model is improved in this work and will be explained in the section 2.3.2.

1.2 Objectives

The goal of this thesis is to characterize the telecommunication chain above 100GHz. Through simulations, a trade-off will have to be made between the number of operations (the power complexity) and the performance recorded in Signal to Noise Ratio (SNR) to obtain a Bit Error Rate (BER) of 10^{-3}, 10^{-4}, and 10^{-5}. The number of operations of the Digital Processing blocks will be determined to estimate the power consumption of the chain with regards to the power consumption per operation. This will then lead to seeing which blocks need to be changed/optimized or for which block reducing the quantization level would be enough.

In this work, the digital Base-band communication part of the power model [10] from IMEC is refined and simulations related to the performance of the quantization are analyzed.

The thesis is organized as follows. In chapter 2, the telecommunication chain used will be explained. We will also explain the methodology to study the power

consumption and the performance. In chapter 3, all the blocks of the chain will be thoroughly looked into and given their number of operations.

In the chapter 4, the simulation results for several scenarios will be assessed.

Finally, in chapter 5, we will summarize our findings and discuss the future prospects of improvements.

2 BLOCK DIAGRAM & METHODOLOGY

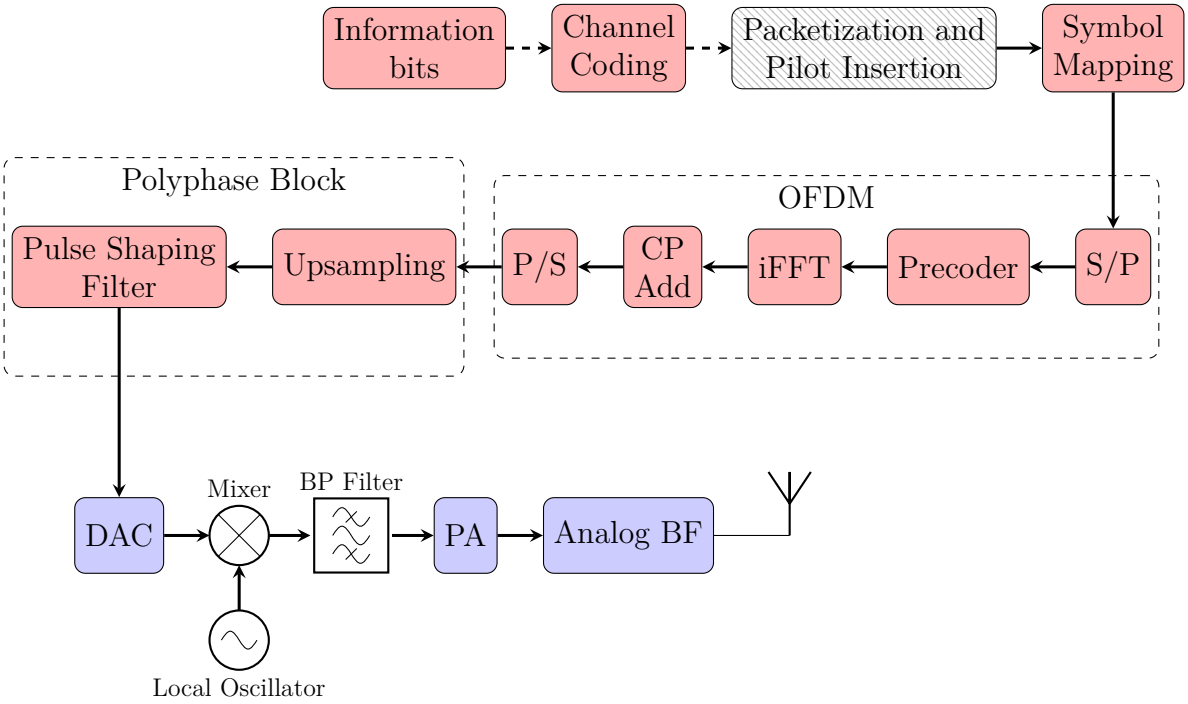

Figure 2.1: Block Diagram: Transmission

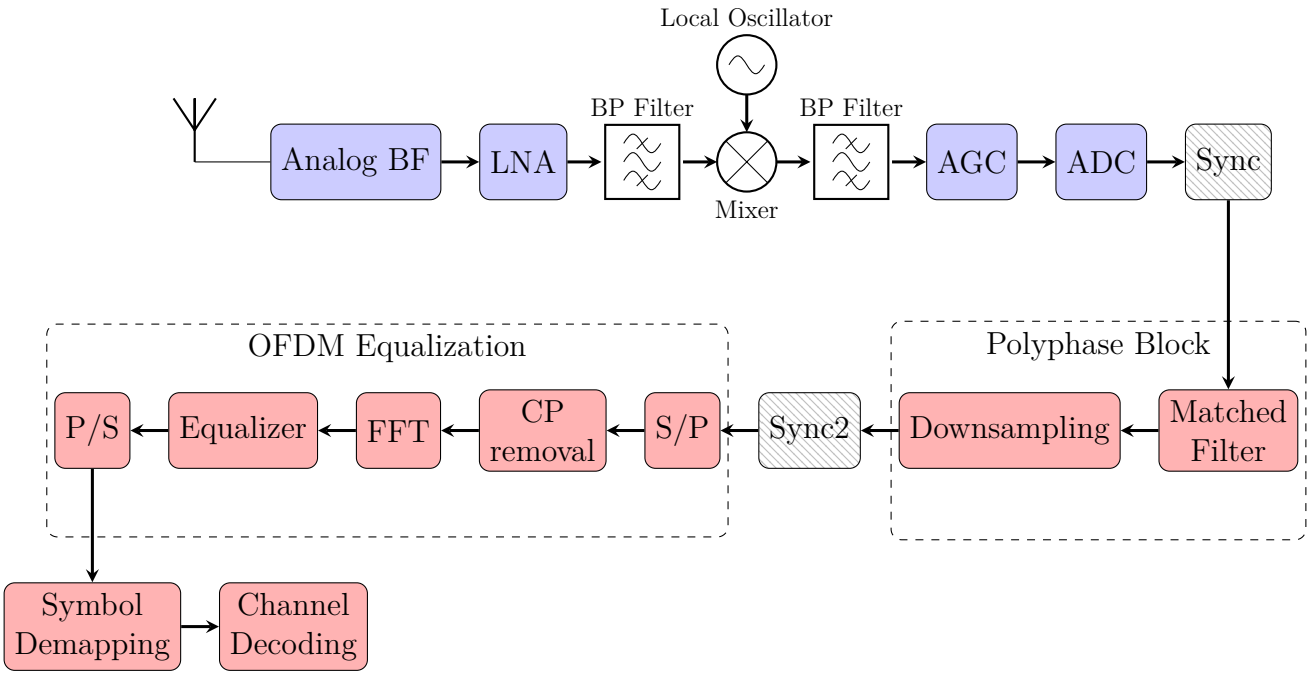

Figure 2.2: Block Diagram: Reception

Here above on the figures 2.1 and 2.2, are the block diagram of the transmission(TX) and the reception(RX) for millimeter-Wave(mm-Wave) frequency communication. In this work, the synchronization is supposed to be perfect (without frequency offset, sampling clock offset, IQ-imbalance, and phase noise). In this chapter, the block diagram of the radio-frequency(RF) communication chain will be explained. In section 2.1, the transmission will be described, and the reception in section 2.2. After, the modelization of the power consumption will be described in section 2.3 with the previous model and the one from this work. And finally, how to link it with the performance in the section 2.4.

2.1 Transmission

Generically, at the transmission, the data sent are sequences of bits of information. They go through a coding block that adds redundancy in the sequence to

balance/counter the effect of the channel. It is also there to correct the effect of the noise and other impairments which could lead to an error in the received bits.

In a simulation scenario with synchronization impairments, known pilots can be included in the packets and sent. These pilots will help to estimate these impairments. Then they would be compensated to recover the signal sent. In this work, only the channel impairments were taken into account such as the random phase due to the distance or the multipath channel with Rician fading [22]. Because of the properties of very high frequencies with heavy path loss, most simulations will be done with a Line of Sight (LoS) component only [32]. In the simulations, the channel impairments such as the phase and amplitude of all the multipaths are known to both TX and RX (meaning perfect estimation) because no estimation algorithm is implemented (none pilots are sent). This would therefore correspond to a perfect channel estimation.

Then the bits are mapped onto the symbols and these constellation symbols will be modulated using OFDM [37]. The modulation operation is the block that changes the digital information into a waveform that can go over a channel(RF in this case). The idea behind OFDM is the following. Each of the symbols will be multiplied to a sine function at a certain multiple of a frequency. Thanks to the orthogonality of sine, they are all orthogonal between each other. This corresponds to a frequency division multiplexing(FDM) by mapping each constellation symbol (for the size of the OFDM symbol) on a subcarrier. And this operation is very similar to an inverse Discrete Fourier Transform (IDFT). So practically, for 1 OFDM symbol, a vector of constellation points corresponding to the subcarriers is put in an IFFT. And that gives a time domain signal which is the addition of all the carriers. And the number of the subcarriers is the same as the length of the OFDM symbol generated.

Then a copy of the last portion of the OFDM symbol is put at the beginning of the OFDM symbol. This is the cyclic prefix and it is used to combat all the discontinuities that happen on the data because of a multipath fading channel. The cyclic prefix will be discarded to remove the effect of the delayed versions of the OFDM symbol before recovering the data. OFDM will thus allow the delay spread to be much longer than if the constellation point were sent. This prevents the ISI from happening.

For mm-Wave frequency, the Non Line of Sights (NLoS) components are more absorbed by the reflectors and the propagation for longer distances will be more attenuated. This means that the cyclic prefix can be shorter. Additionally, due to the BeamForming, the energy will not be directed in the direction of the reflector resulting in a smaller effect of the reflected part.

For a MIMO situation, a precoder can be added to help the beamforming of the signal to put all the energy in the direction of the user and nulls for the direction of other users for example. This precoder can be of several types: Zero Forcing(ZF), maximum combining transmission(MCT), and minimum mean square error(MMSE) and they will be more explained in the section 3.8.

The signal can also be upsampled or not if guard bands are used instead. If the signal is not upsampled, the Nyquist theorem shows that aliasing will appear. The guard bands in OFDM are needed and have the same effect in this case. The zero padding in the frequency domain is in fact an oversampling in the time domain. And so no data is read on the corrupted bands.

The signal goes through a pulse shaping filter that, as the name says, shapes the signal in a way to limit the usage of the bandwidth.

After all the digital processing, the signal goes through a digital-to-analog converter (DAC) and then in the case of Radio Frequency (RF) communication, goes through the mixer to transmit the signal around the carrier frequency. The signal is then amplified before being sent to the antenna.

2.2 Reception

At the reception, first, the signal needs to be also amplified with a Low-Noise Amplifier (LNA) because of the attenuation due to the distance between the TX-RX antennas. Then it goes through a Band-pass filter to filter out all the part of the spectrum which is not part of the signal of interest. Then it goes through the mixer to go back to the baseband. After, the Automatic Gain Control(AGC) will work with the Analog-to-Digital Converter to maximize the usage of the ADC so that it does not saturate and that it has an optimal dynamic range.

Then the synchronized signal in this case goes through a matched filter which maximises the SNR.

The cyclic prefix of the OFDM symbols is removed and the FFT is performed to get back the subcarriers with as values the constellation points. But before getting the symbol demapping, equalization needs to be performed to remove the effect of the channel on the streams. After that, the symbol demapping is done with a soft-decision to enter the channel decoding.

2.3 Power Modelization

The methodology to characterize the power consumption of each scenario was to say that the power consumption comes from several different parts. There is the analog part including the PA, and all the other analog components (such as Low-Noise Amplifier, Local Oscillator, mixers, Band-pass and low-Pass filters). There is also the digital part which will be updated from the previous model. And the last part is the general system overhead which corresponds mostly to the losses of the supply [10]. The previous and the new model will be explained in this section.

A big part of the power consumption of the whole system is due to the PA as it increases the power of the signal to be sent at the antennas[1]. Its power consumption depends on the internal efficiency of the PA and the output power needed for the operation point. And for sub-terahertz frequency designs(from 100GHz), the maximum power efficiency for a 300GHz power amplifier is 7% with a 11mW output power[13]. Then the other analog components are modeled from the state of the art. The losses from the overhead/supply that are taken into account are due to the power converters with 8% of losses. The modelization of these parts was taken from previous research from IMEC [10].

2.3.1 Description previous model

In the previous model[10], the power consumption of the digital part of the communication was computed by counting the number of operations. The number of operations of each block depends on several factors: the modulation, the bandwidth used, the size of the FFT block,...). This represents the complexity. For each block, a different quantization level could be used and so the complexity of each block has to be multiplied by a quantization scaling. The scaling was approximated to 1.2, as more linear operations were done than quadratic. This power model took only the basic operations such as additions and multiplications and no memory so a factor of overhead of 2.5 was needed. To translate these numbers of operations in terms of power consumption, it needs to be multiplied by an energy efficiency for a certain reference technology. The one from the paper is 300GOPs/W for 4-bit complex operations in the 28nm technology. The formula can be seen below.

$$
\begin{aligned}
\text{Power Consumption} = {} & \text{Complexity} && \text{(scaled with bandwidth, number of streams, modulation,...)} \\
& * \text{ Quantization scaling} && \text{(Power factor : different per operation)} \\
& * \text{ Overhead} && \text{(memory operations, flexibility)} \\
& / \text{ Efficiency} && \text{(GOPS/W for reference technology)}
\end{aligned}
$$

2.3.2 New Model

In this work, the consumption of power for the digital part of the communication is also based on the previous model. As in the previous model, the complexity is computed on each block separately to count the number of operations. But each type of operation is counted individually, including the number of additions (add), the number of multiplication with a constant value ($mult_{cst}$), the number of multiplication of 2 variables ($mult_{var}$), the number of Look-Up Tables accesses (LUT) and the number of memory accesses for both reading and writing (Mem). A distinction between the 2 types of multiplication is done because the design architecture can be optimized if the multiplication factor is known in advance. This can create a path to decrease the complexity of the multiplication drastically. With all the operations taken differently, their power consumption will also need to be computed separately.

In the communication chain, in between the Symbol Mapping block and the Channel decoding block(in the case of a soft Symbol demapper), the samples are represented/quantized with more bits. Thus the number of operations to perform an addition for example will be bigger.

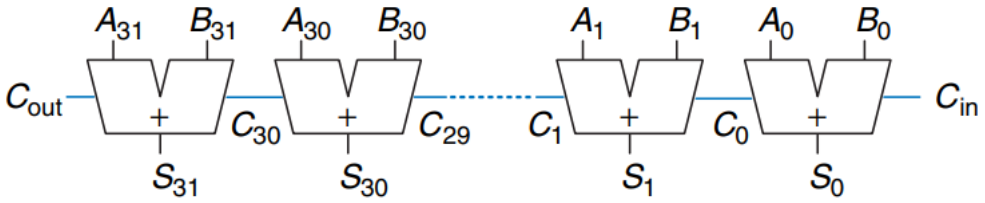

Figure 5.5 32-bit ripple-carry adder

Figure 2.3: Example Full-Adder 32 bits [15]

Figure 2.3 illustrates that the N-bit adder can be done by chaining together N full-adders. This increase linearly the consumption with regard to the number of bits. In consequence, each operations are closely related to the number of bits used so the quantization level has here an impact on the energy consumption.

For each access to memory or operation such as additions or multiplication, an energy per bit is considered. This energy is evolving with a linear scale for operations as additions or for memory access and a quadratic scale for multiplication. For example, for a multiplication of 2 4-bit variables, there will be a power consumption of $cst.4^2$ fJ and for an addition this comes down as $cst.4$ fJ. The energy constant cst

will determine what is the energy consumption for this type of operation. Curves of energy per operation per bit have been made thanks to this paper [18].

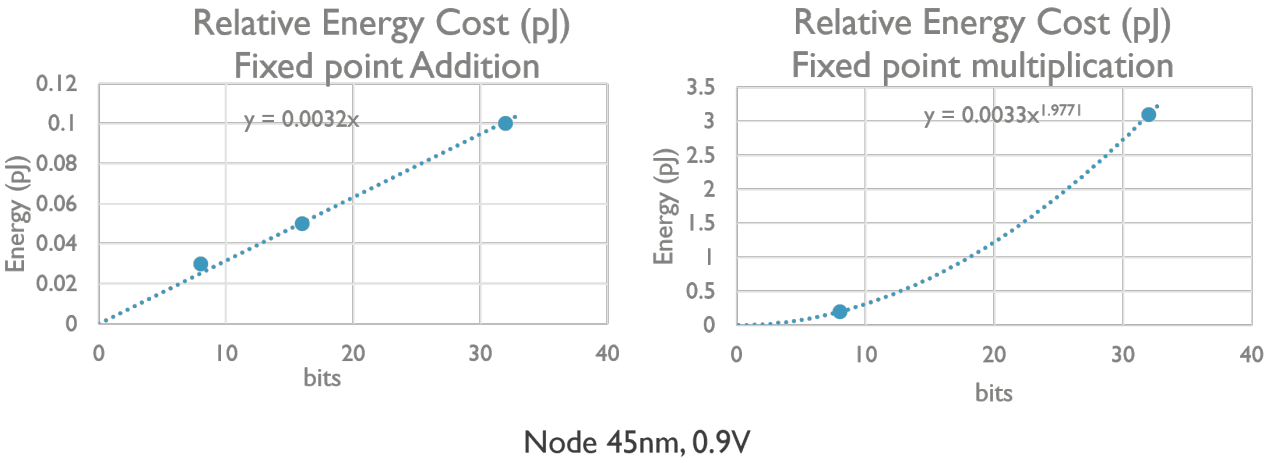

Figure 2.4: Energy per Addition and Multiplication

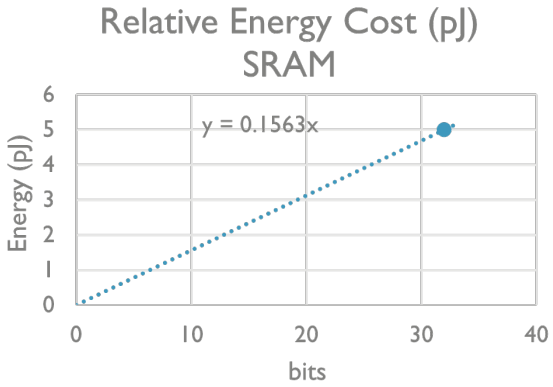

Figure 2.5: Energy per memory

The Figures 2.4 2.5 illustrate the energy functions of the operations with the bits representation of the data. Because of the few data points provided, the values of the constants are rough estimations. We estimate then that the power factor of the multiplication should have been 2 and the other constant should have been the same as for the addition.

The memory is read or written normally per word(32-bit) and not per bit so normally we should not describe the energy consumption per bit for this operation. But as multiple operations can be processed at the same time, multiple data(represented with 8bits for example) can be read at the same time in one 32-bit word to be further processed. We can therefore also do an estimation per bit of the memory. The figure also shows that the energy of the SRAM is 50 times superior to the addition.

The values of the constants are also on the graphs for a technology on 45nm. To have the estimation of the energy for 7nm (2022 - product), we have to multiply the constant by the power saving factor of 0.0528 related to the year technology ($= 0.5^3 0.65^2$) [10].

For example, if we want to perform 10 additions and 11 multiplications with 8-bit representation we will have the following formula for the energy consumed for these operations:

$$\text{Energy} = (10 * 0.0032 * 8 + 11 * 0.0032 * 8^2) * 0.0528 = 0.132 \ \ [\text{pJ}]$$

Returning to the link with the previous model, no overhead should be needed in this case as the memory is taken into account. And because we get the energy of the operation directly, it just needs to be multiplied by the frequency at which this operation is performed.

The global power consumed is thus the sum of all the blocks of the power consumed by each block. And the power on one block is the energy of all the operations in this block multiplied by their frequency of activation.

The estimated power result is therefore in this equation :

$$\text{Power Consumed} = \sum_{blocks} \left(\sum_{Ops} (\sigma \ \varepsilon(\text{bits})) \ \chi f_{co} \right) \tag{2.1}$$

With σ the number of a certain type of operation for a certain block (Ops being all the types of operations), ε(bits) the energy constant of this operation for a data represented over a certain number of bits, χ the number of activation per constellation symbol of this block and f_{co} the constellation rate.

The power to access lookup tables was neglected in the results afterward. And the two types of multiplications were considered the same.

2.4 Performance Simulations

The chain is simulated in MATLAB to observe the performance with regard to the quantization level of the different blocks. In the simulation, the inputs of each block (fft,...) are quantized to a certain level. Then in the block, the operations are not quantized and only the output is. The inside of the blocks is considered a black box in terms of quantization.

The quantization level used for each block impacts the performance of the communication. A lower number of quantization levels will add more distortion to the signal hence decreasing the BER. A lower number of quantization levels will thus decrease the performance but also decrease the power consumption as seen in the subsection 2.3.2. The performance in terms of the power of the Digital part estimate and the SNR to achieve a specific BER(=1e-5,1e-4,1e-3) is recorded for some scenarios with varying quantization levels. Then all these different points of performance for quantization setups are put in a plot to see which combination of quantization levels for each block is optimal for the scenario.

This will be done at first only on the digital part of the chain to see the improvements and then at the end also with the analog part to see the global power.

3 BLOCKS AND ALGORITHMS

In this chapter, we analyze the digital blocks of the communication chain with their algorithms. The number of operations is computed for all the blocks.

We also analyze the Beamforming and the channel model used for MU-MIMO simulations.

3.1 Channel Coding

The information bits are coded to introduce redundancy in the chain. It allows to have correcting capabilities if some bits are corrupted by the channel. The channel decoder will be able to correct the errors if the number is reasonable.

For high data rates, the most used code is LDPC-coding[23] because they require low decoding complexity but with long block lengths. On the other hand, Turbo-codes require a higher decoding complexity than LDPC-codes and can achieve good performance even with smaller block lengths[16].

As the goal is to transmit data rates in the range of tera-bits, LDPC is chosen. It is also the most common type of coding currently used for 5G standards[11].

The coding is implemented using a sparse matrix-vector multiplication. Normally, the matrix given is the parity-check matrix and it is given with a base matrix that has to be extended [40].

$$B = \begin{bmatrix} 2 & -1 & 1 & 3 & 0 & -1 \\ 1 & 0 & -1 & 0 & 0 & 0 \\ -1 & 3 & 2 & 1 & -1 & 0 \end{bmatrix}$$

Base graph **B**

$H =$ 

Parity-check matrix **H**

Figure 3.1: Example : Base Matrix - Parity Check Matrix [40]

Figure 3.1 shows how the base matrix is represented and expended to create the Parity check matrix. This base matrix is given with an expansion factor equal to 4. The value -1 corresponds to a zero matrix and all other values of the base matrix correspond to circular shifts on the rows of the identity matrix.

As we want to optimize the power of the communication, we choose the parity-check matrix, and from that it is possible to transform this matrix into its generating matrix. This way, for a given code rate, simpler computations are used to generate the coded bits.

$$\mathbf{c} = \mathbf{b}\,\mathbf{G}$$

$$\begin{bmatrix} c_1 & \dots & c_{N_{codedbits}} \end{bmatrix} = \begin{bmatrix} b_1 & \dots & b_{N_{infobits}} \end{bmatrix} \begin{bmatrix} G_{1,1} & \dots & G_{1,N_{codedbits}} \\ \dots & \dots & \dots \\ G_{N_{infobits},1} & \dots & G_{N_{infobits},N_{codedbits}} \end{bmatrix}$$

With **c** the coded bits, **b** the information bits, and **G** the generating matrix of the LDPC code.

For each coded bit, there are $N_{infobits}$ additions modulo 2(XOR operations). But because we know the generating matrix, only the indices of the ones in the generating matrix are considered. This will thus give the number of operations(only additions) of the coded block that is equal to the number of ones in the generating matrix. And for the memory, all the bits read are stored in the registers at a negligible cost and the coded bit is written on the memory.

Each coded bit has an average layer degree number of additions.

$$\begin{aligned} \#Op &= (D-1)\ add && [/\text{coded bit}] \\ \#Mem &= D[\text{read}] + 1[\text{write}] && [/\text{coded bit}] \end{aligned}$$

Where D is the LDCP layer degree which corresponds to the mean number of ones per column in the generating matrix.

If we want to relate it to the activation at the symbol rate, $\log(M)$ coded bits needs to be created for one symbol. The number of operations is therefore done $\log(M)$ times per symbol with M being the modulation Order.

The coding rate will impact the LDCP layer degree and most of all, the overall power consumption if we speak in terms of information data rate.

3.2 Channel Decoding

The channel decoding block is the block that uses the channel outputs to provide an estimation of binary inputs. In this work, the channel output is the output of the soft demapper discussed in section 3.4. The decoding used for the LDPC is an iterative algorithm known as the Sum-Product Algorithm(SPA) (also known as belief propagation algorithm) [21] [23]. It works globally as follows: the variable nodes send soft-information messages to the check nodes. These messages correspond to the probabilities for the check nodes to be "1" or "0" based on the received data and previous "check-to-variable" messages. Then the check nodes compute the "check-to-variable" messages by combining the incoming "variable-to-check" messages. Then, the new probabilities for the transmitted bits are computed. These steps are done for several iterations until convergence to a bit sequence or the maximum number of iterations is reached. The Min-Sum Algorithm can be seen as a simplified logarithmic SPA [36]. The number of operations is related to the number of check nodes and variable nodes of the LDPC code. But also to the number of iterations needed to converge. It is approximated to the following formula

$$\#Op = \iota * D[add]$$
$$\#Mem = \iota * D[add]$$

Where ι is the number of iterations and D the LDPC layer degree.

In this block compared to the channel coding block, the quantization level (Q) used is not 1 but bigger to represent all the probabilities values. And the number of activation per constellation rate is the same as for the channel coding: $\log(M)$.

3.3 Mapping

The mapping is the operation done to transform the array of bits in constellation symbols. The mapping used for most transmissions is the quadrature amplitude modulation(QAM) with gray coding. The gray-coding is a technique to arrange the binary values of a symbol so that only one bit of difference appears between neighboring symbols. The QAM is usually chosen because of its high spectral density which allows it to transmit much data over a given bandwidth. However, its performance degrades rapidly in the presence of channel impairments. These are corrected by using equalization, synchronization, and interference cancellation.

The implementation of the mapping can be done easily by reading the bits by block and assigning them to Look-Up-Table(LUT).

For example, for 16-QAM the bits are read by 4 and this value is the index of the LUT which will then write the value of the symbol. Figure 3.2 shows the gray mapping of the 16-QAM and how the bits are transformed into symbols.

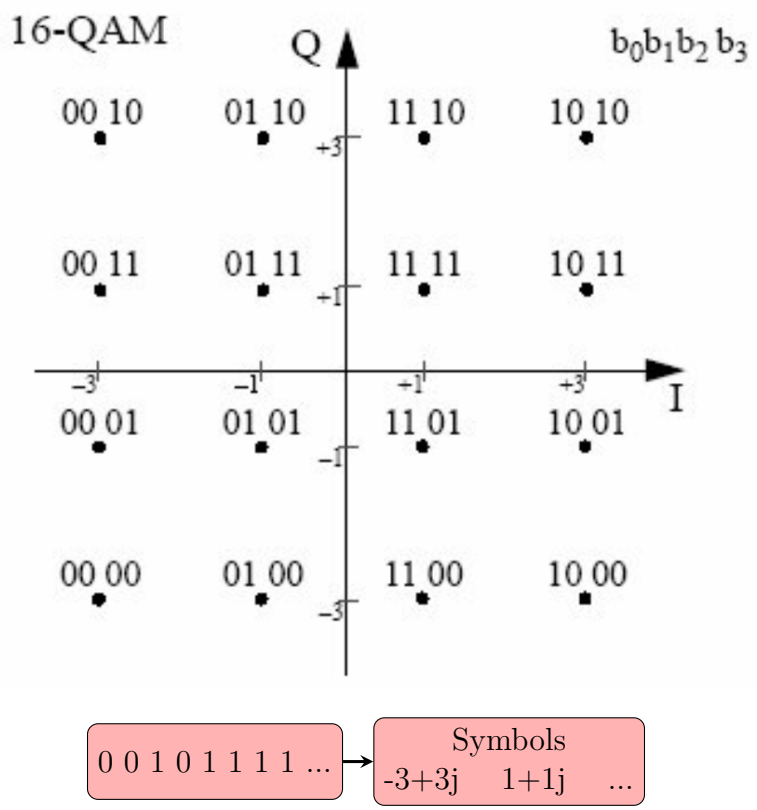

Figure 3.2: Mapping [41]

The number of operations done is:

$$\#Op = 1\text{LUT}$$
$$\#Mem = \log(M)[\text{read}] + 2Q[\text{write}]$$

In the equation for the memory, Q is the quantization level of the symbol, and 2 is therefore to count for both I/Q components. This equation shows that at the entry of the block, the data is read on the bits and after the block, the symbol is written on the symbols that are represented on Q bits.

The activation is of course 1 by constellation rate.

3.4 Demapping

The demapping change with the modulation used and can be with a soft or a hard decision. Soft demapping allows us to take the degree of certainty of the

symbols but needs more computational resources. For QAM, the soft demapping was developed in an internal research from IMEC [9].

In the soft-output demappers, the goal is to compute the Log-Likelihood Ratio(LLR) instead of a hard-decision decoding.

So for c_i, the coded bit i, the formula for LLR says :

$$c_i = \log\left(\frac{\sum_{S_1} p(s_i)}{\sum_{S_0} p(s_i)}\right)$$

Where $S_{0/1}$ are the set of constellation points for which the i^{th} bit is 0/1 and $p(s_i)$ is the a-posteriori probability. Because of the independence of the noise and the mapping for both the in-phase component and the in-quadrature component for QAM, only the I component was analyzed further. This equation can therefore be simplified as follows :

$$c_i = \log\left(\frac{\sum_{I_1} \exp(-\frac{(I_i - r_I)^2}{2\sigma_n^2}}{\sum_{I_0} \exp(-\frac{(I_i - r_I)^2}{2\sigma_n^2}}\right)$$

Where I_i and r_i are the real components of the set of values and of the received signal.

This formula can be linearized per piece. Hereunder is an example of the 16-QAM for the first 2 bits only representing the real component of the symbol. The same formulas can be used for the 2 other bits.

$$\begin{aligned}
c_1 &= 4\frac{(r_I + 1)}{\sigma_n^2} && r_I \leq -2 \\
c_1 &= 2\frac{r_I}{\sigma_n^2} && -2 \leq r_I \leq -2 \\
c_1 &= 4\frac{(r_I - 1)}{\sigma_n^2} && 2 \leq r_I \\
c_2 &= 2\frac{(r_I + 2)}{\sigma_n^2} && r_I \leq 0 \\
c_2 &= -2\frac{(r_I - 2)}{\sigma_n^2} && 0 \leq r_I
\end{aligned}$$

We can see from these formulas that one addition and one multiplication by a variable is performed but there are also $\log(M)$ if conditions to see in which zone is the sample received. The if-conditions are considered as additions.

$$\#Op = \log_2(M) mult_{var} + 2\log_2(M) add$$
$$\#Mem = 2[\text{read}] + \log_2(M)[\text{write}]$$

This operation is done on Q bits and is done once per constellation rate with Q being the quantization level (number of bits) of this block.

3.5 FFT/IFFT

To go from the frequency domain to the time domain or reversely, the Fourier or inverse Fourier transform is needed to perform. And because the signals are discreet, the Fourier transform is a Discreet Fourier Transform. The formula of this algorithm is the following

$$X(k) = \sum_{n=0}^{N-1} x[n] \exp\left(jn\frac{2\pi}{N}k\right)$$

This formula can be executed in $O(N^2)$ for all signals but a better algorithm was found exploiting the symmetries of complex exponential. It is called the Fast Fourier Transform(FFT).

Figure 3.3 shows an example for the FFT algorithm on a block size=8.

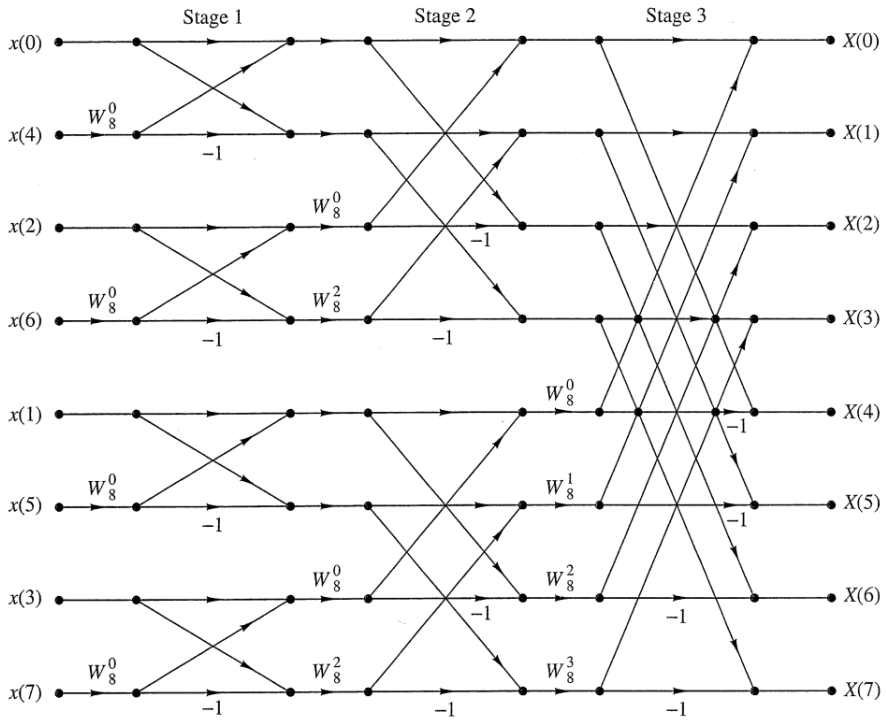

Figure 3.3: 8-point decimation-in-frequency FFT algorithm [31]

See the appendix A for the implementation.

Also multiplication and the additions of 2 complex numbers, $mult_{\mathbb{CC}}$ and $add_{\mathbb{CC}}$, can be decomposed in terms of real additions and real multiplication with the following formula :

$$\begin{aligned} mult_{\mathbb{CC}} &= 4mult + 2add \\ add_{\mathbb{CC}} &= 2add \end{aligned}$$

This type of algorithm allows to change the complexity of the operation for the FFT block from $O(n^2)$ to $O(n \log_2 n)$ with the FFT block being the N samples going into the FFT algorithm. The number of operations for 1 FFT block is

$$\begin{aligned} \#Op &= \log_2(N)\frac{N}{2}mult_{\mathbb{CC},cst} + \log_2(N)Nadd_{\mathbb{CC}} && \text{[/FFT block]} \\ \#Op &= \log_2(N)2Nmult_{cst} + \log_2(N)3Nadd && \text{[/FFT block]} \\ \#Op &= \log_2(N)2mult_{cst} + \log_2(N)3add && \text{[/sample]} \end{aligned}$$

And for the memory, we access the data at each multiplication for both I and Q components so it becomes :

$$\#Mem = \log_2(N)N[\text{read}] + \log_2(N)NLUT + \log_2(N)N[\text{write}] \quad [/\text{FFT block}]$$
$$\#Mem = 2\log_2(N) + \log_2(N)LUT \quad [/\text{sample}]$$

This operation is done at the same rate as the constellation rate on Q bits where Q is the quantization level of this block.

3.6 Up(/Down)sampling And Filtering

Upsampling and downsampling the signal allows us to use the whole bandwidth available (Nyquist theorem). The signal needs to be filtered after to not encounter aliasing.

Thanks to polyphase components, the filtering can be done during the up/downsampling. This allows filtering at the lower rate of the signal, decreasing the number of operations and therefore, its power consumption.

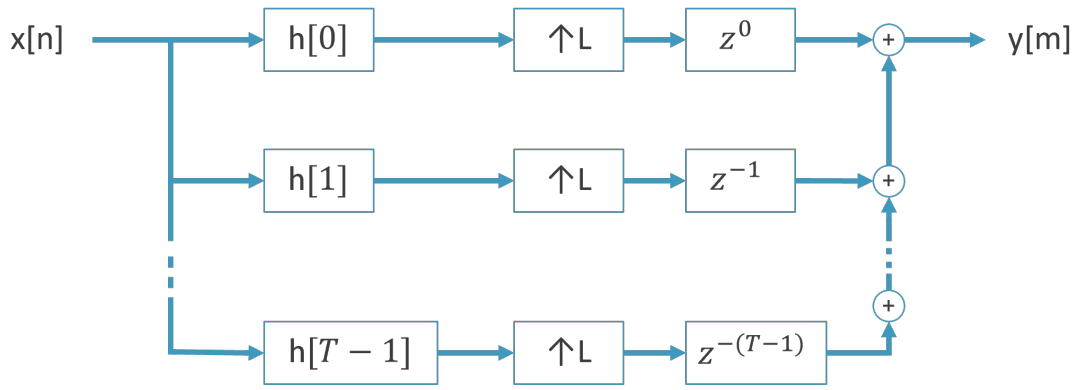

Figure 3.4: Upsampling and filtering in one block

Figure 3.4 shows how the upsampling and the filter would be implemented in one block. T is the number of taps of the filter and L is the upsampling factor. The rate of the output is therefore L times bigger.

For a real($\mathbb{R}$) filter, we have the following number of operations :

$$\#Op = (T mult_{\mathbb{CR},cst} + (T-1)add_{\mathbb{CR}})/L = (2T\ mult_{cst} + 2(T-1)add)/L \quad [/\text{oversample}]$$
$$\#Mem = 2\frac{T}{L}[\text{read}] + 2[\text{write}] \quad [/\text{oversample}]$$

This block is done L times per constellation rate also on a certain quantization Q.

3.7 Channel Estimation

Channel Estimation is a crucial block of the communication chain. Its main function is to estimate the characteristics of the channel to be able to compensate for these effects. The compensation is done on the equalizer and if the system is MIMO, a precoder can be added at the transmitter too. To estimate the channel, known symbols are sent on the preamble[24]. The estimation is done once per packet. This block was not put in the simulation.

Because of the multipath properties of the channel. The channel can be modeled in the time domain with several delay taps. The signal at the reception is therefore a convolution on all the channel taps of the signal sent. In the frequency domain, this corresponds to just one multiplication per subcarrier. This operation will therefore be computed in the frequency domain as OFDM is perfectly suited for this. If we assume that the channel is flat on a coherent bandwidth(corresponding to N_c subcarriers), we can estimate it using just a division with the pilot sent.

$$\#Op = 1mult_{\mathbb{CC}}/N_c = (4mult_{cst} + 2add)/N_c \quad [/\text{subcarrier}]$$

The rate of the subcarriers is the same as the constellation rate.

But to mitigate the effect of the noise on the estimation, a smoothing FFT can also be included. The channel frequency response is transformed in the Time domain. There, the noisy taps are discarded and an FFT is used to go back to the frequency domain. This corresponds to 2 FFT operations.

$$\#Op = 2\#Op_{FFT} = 2(\log_2(N)2mult_{cst} + \log_2(N)3add) \quad [/subcarrier]$$

3.8 MU-MIMO Precoding

The precoder is applied at the transmission for a MU-MIMO simulation. It is used to take advantage of the multiple antennas to increase the quality of the signal at the receiver by reducing the interference between the users that occurs on the wireless channel. By doing so, it allows to take the spatial dimension of the users to do a spatial multiplexing of their signal.

For OFDM, this operation is done in the frequency domain. And this has the advantage that it can help maximize the allocation of resources in the case of a frequency-selective channel for example. In that case, a certain subcarrier will not be able to transmit very well due to the frequency selectivity of the channel. The precoder will therefore enhance the spectral efficiency.

The precoding matrices that are tested are Zero-Forcing (ZF) and Maximum Combining Transmission (MCT) sometimes also known as Maximum Ratio Transmission (MRT) [19]. For the MCT, the precoding matrix is the hermitian(conjugated and transposed) of the channel matrix. No computation needs to be performed before the data is precoded. The matrices on which these operations are performed are of size: $N_s \times N_s$, with N_s being the number of users based on the channel model developed in the section 3.12.

For the Zero-Forcing, the channel estimation matrix needs to be inverted. To do this, the Gauss-Jordan method is used. It consists to triangularise the matrix first in an Upper Triangular Matrix and then perform the Upward pass to have an Identity matrix at the end. The same operations are executed in parallel on an Identity matrix and the result will therefore be the inverse matrix ($[A|I]$ becomes $[I|A^{-1}]$) [8].

On the downward pass, for one row, there is the following number of operations for a matrix $n \times n$. The variable n is the number of streams N_s in this case.

$$
\begin{array}{c}
1 \\ 2 \\ \vdots \\ i-1 \\ i \\ i+1 \\ \vdots \\ j \\ \vdots \\ n
\end{array}
\left(\begin{array}{cccccccc|cccccccc}
1 & x & ... & x & x & x & ... & x & x & 0 & ... & 0 & 0 & 0 & ... & 0 \\
0 & 1 & ... & x & x & x & ... & x & x & x & ... & 0 & 0 & 0 & \cdots & 0 \\
\vdots & & \ddots & & \vdots & & \ddots & \vdots & \vdots & & \ddots & & \vdots & & \ddots & \vdots \\
0 & 0 & \cdots & 1 & x & x & \cdots & x & x & x & ... & x & 0 & 0 & \cdots & 0 \\
0 & 0 & \cdots & 0 & c & x & \cdots & x & x & x & ... & x & 1 & 0 & \cdots & 0 \\
0 & 0 & \cdots & 0 & x & x & \cdots & x & x & x & ... & x & 0 & 1 & \cdots & 0 \\
\vdots & & \ddots & & \vdots & & \ddots & \vdots & \vdots & & \ddots & & \vdots & & \ddots & \vdots \\
0 & 0 & \cdots & 0 & d & x & \cdots & x & x & x & ... & x & 0 & 0 & \cdots 1 \cdots & 0 \\
\vdots & & \ddots & & \vdots & & \ddots & \vdots & \vdots & & \ddots & & \vdots & & \ddots & \vdots \\
0 & 0 & \cdots & 0 & x & x & \cdots & x & x & x & ... & x & 0 & 0 & \cdots & 1
\end{array}\right)
$$

Downward Pass	Add	Mult (and div)	number of times
$R_i \Longrightarrow cR_i$	0	n	1
$R_j \Longrightarrow R_j - dR_i$	n	n	n-i

Over all the rows, it correspond to :

$$\#Add = \sum_{i=1}^{n}(n-i)n = n^3 - n\sum_{i=1}^{n} i = n^3 - n\frac{n(n+1)}{2} = \frac{1}{2}n^3 - \frac{1}{2}n^2$$
$$\#mult = \sum_{i=1}^{n}(n + n(n-i)) = \frac{1}{2}(n^3 + n^2)$$

And for the Upward pass :

$$\begin{array}{c} 1 \\ 2 \\ \vdots \\ i-1 \\ i \\ i+1 \\ \vdots \\ j \\ \vdots \\ n \end{array} \left(\begin{array}{cccccccc|cccccccc} 1 & x & ... & x & x & 0 & ... & 0 & x & x & ... & x & x & x & ... & x \\ 0 & 1 & ... & x & x & 0 & ... & 0 & x & x & ... & x & x & x & \cdots & x \\ \vdots & & \ddots & & \vdots & & \ddots & \vdots & \vdots & & \ddots & & \vdots & & \ddots & \vdots \\ 0 & 0 & \cdots & 1 & x & 0 & \cdots & 0 & x & x & ... & x & x & x & \cdots & x \\ 0 & 0 & \cdots & 0 & 1 & 0 & \cdots & 0 & x & x & ... & x & x & x & \cdots & x \\ 0 & 0 & \cdots & 0 & 0 & 1 & \cdots & 0 & x & x & ... & x & x & x & \cdots & x \\ \vdots & & \ddots & & \vdots & & \ddots & \vdots & \vdots & & \ddots & & \vdots & & \ddots & \vdots \\ 0 & 0 & \cdots & 0 & 0 & 0 & \cdots 1 \cdots & 0 & x & x & ... & x & x & x & \cdots & x \\ \vdots & & \ddots & & \vdots & & \ddots & \vdots & \vdots & & \ddots & & \vdots & & \ddots & \vdots \\ 0 & 0 & \cdots & 0 & 0 & 0 & \cdots & 1 & x & x & ... & x & x & x & \cdots & x \end{array}\right)$$

Upward Pass	Add	Mult (and div)	number of times
$R_j \Longrightarrow R_j - dR_i$	n	n	n-i

$$\#Add = \#mult = \sum_{i=1}^{n}(n-i)n = \frac{1}{2}n^3 - \frac{1}{2}n^2$$

The total number of additions and multiplications to find the inverse are the following :

$$\#Add = 2\,(\frac{1}{2}n^3 - \frac{1}{2}n^2) = n^3 - n^2$$
$$\#mult = \frac{1}{2}(n^3 + n^2) + \frac{1}{2}n^3 - \frac{1}{2}n^2 = n^3$$

This is done for a complex matrix so the multiplications and the additions need to be modified accordingly.

$$\begin{aligned} \#Op &= 4(n^3)mult + (2(n^3) + 2(n^3 - n^2))add \\ &= (4n^3)mult + (4n^3 - 2n^2)add \end{aligned}$$

This inverse is calculated on all the subcarriers. But we can suppose a coherent bandwidth so that the channel in this bandwidth is considered flat. This means that the inverse can be computed once every N_c (the coherence BW in terms of subcarriers).

$$\#Op = ((4N_s^3)mult + (4N_s^3 - 2N_s^2)add)/N_c \qquad [/\text{subcarrier}]$$

It is then applied to all the subcarriers of the data.

$$\#Op = N_s mult_{\mathbb{CC},var} + (N_s - 1)add_{\mathbb{CC}} = 4N_s mult_{var} + (4N_s - 2)add \quad [/\text{subcarrier}]$$

3.9 Equalisation

Equalization is the block used to compensate at the reception for the distortion introduced by the channel. Because the goal is to transmit at a high data rate and with low power, linear equalizers are preferred compared to non-linear ones which require more computational resources.

There are many different algorithms for equalization, the most known are the Zero-Forcing (ZF) and Minimum Mean Square Error (MMSE). Only the ZF equalizer was used for the simulations. In the case of a MU-MIMO simulation, we also suppose that the receptor has only knowledge of his channel with the transmitter and not the channels of other users.

The computation of this is the following :

$$\#Op = 1mult_{\mathbb{CC},var} = 4mult_{var} + 2add \quad [/\text{subcarrier}]$$

This corresponds to the inverse operation of the channel estimation and this weight calculation is done once per preamble so once per packet.

And 1 complex multiplication is also done on all the subcarriers to equalize the signal. This is done on all the data.

3.10 Synchronisation

Even if the synchronization was not implemented and tested, some algorithms for the synchronization were still analyzed [28].

For the CFO estimation, the first algorithm considered was the one from P.H. Moose. But because IQ imbalance and CFO estimation degrade each other, it would be best to have an algorithm that does the 2 at the same time [12].

A proposed method would be to first estimate roughly the CFO with the Moose algorithm and sampling clock offset with an interpolation in the first synchronization block. This block is done before the downsampling so it is at a higher rate to find a first rough correction. After that, more complex algorithms could be used at a lower rate to find the estimation and compensate for the joint effect of IQ imbalance and CFO and the phase noise.

The Moose Algorithm is a data-aided algorithm sending repetitive blocks so that the difference between the consecutive blocks shows the offset in frequency [29]. The formula is

$$\hat{\Delta f_c} = \frac{\arg\left(\sum_{l=0}^{N_t-1} y[l+N_t]y^*[l]\right)}{2\pi N_t} f_{OSF}$$

Where $\hat{\Delta f_c}$ is the estimate of the difference in the carrier frequency of TX and RX, N_t the size of the repetition block, and f_{OSF} the sampling frequency including the oversampling factor. To find the argument, the CORDIC(coordinate rotation digital computer) algorithm is used [3].

And the compensation is done also using CORDIC and applied to all the oversampled samples.

The sampling clock offset appears if there is a clock frequency difference between TX and RX. This creates a varying delay in the exact sample timing and to compensate for this effect, an interpolation filter is applied.

$$\#Op = N_{sco}mult + (N_{sco} - 1)add \quad [/\text{oversampled sample}]$$

Where N_{sco} is the number of taps of the interpolation filter.

The second block of the synchronization could be a joint estimation with an expectation-maximization(EM) algorithm performed iteratively on the CFO and the IQ-imbalance [17].

3.11 BeamForming

To increase the spacial diversity and with that, the performance, beamforming is also used. There are 3 types of beamforming possible, analog BeamForming, digital beamforming, and hybrid beamforming. Figure 3.5 shows the three types of beamforming possible.

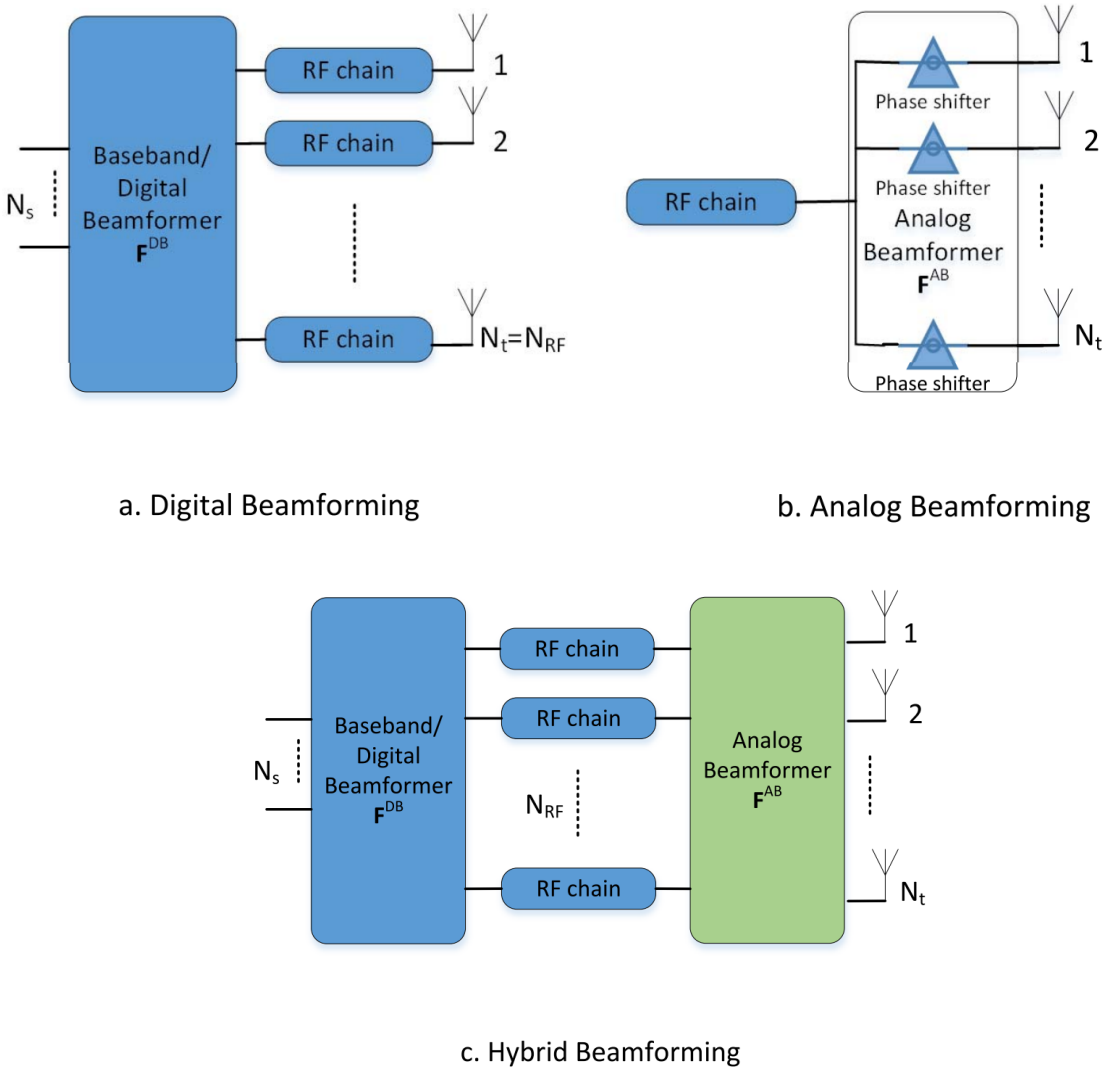

Figure 3.5: Beamforming architectures in mm-Wave massive MIMO systems: (a) Fully-digital architecture, (b) Analog only architecture, (c) Hybrid analog/digital architecture [2]

Analog beamforming is using 1 digital chain for multiple antennas. They combine together to point in a specific direction. The drawback is that the circuit is built for a specific direction and cannot change in time to point at another user for example.

Digital beamforming, on the other hand, means that each antennas receive a separate signal coming from a digital chain. Each signal is digitally precoded in order to maximize the useful signal and minimize the interference between users. For that, it can change the phase and amplitude on each subcarrier of the signal. This one is more flexible because it can be modified regarding the conditions during the communication but it increases the digital complexity and so the power consumption.

Hybrid beamforming is a combination of both analog and digital BF so that packets of antennas are using analog beamforming to steer in a certain direction and digital beamforming will be used considering each packet of antennas as one directive antenna. Analog beamforming is used to create the beamshape to steer the signal in a certain direction and digital beamforming is used to modify the beamshape to have nulls in the other directions of the users.

For the high frequency, known as mm-Wave frequency, Hybrid beamforming will be considered. Because at these frequencies, the antennas are very small, this means that the power they radiate is also small and so, to get the same level of power, many antennas are needed. This has for consequence that for digital BF many PAs would be also needed. To reduce this number while still having adaptability, Hybrid Beamforming is used.

3.12 MU-MIMO Channel Model

For a MIMO system, there are multiple antennas and channels associated to them. Because the antennas are really close to each other, it is supposed that the channel between them is the same, at least for one stream.

If the angle of departure (AoD) is non-zero, there is a delay in the signal at the antennas. The field lines are approximated to be parallel thanks to the Fraunhofer approximation of long distances (far field communication). The delay between the antennas is a function of the distance between the antennas in this case and the phase-shift. The antenna pattern used is a uniform linear array antenna. For this type of array, there exists an array factor to determine the parameters.

$F(\theta, \phi) = \sum a_n \exp(jkr_n.\hat{r}) = \sum_{n=1}^{N} \exp(j\ (n-1)\psi)$ with $\psi = kd(\hat{r}.\hat{u}) + \Phi$ [26].

$$a_n = \exp\left(j(n-1)\Phi\right) \qquad \text{Uniform amplitude and phase difference}$$
$$r_n = (n-1)d\,\hat{u} \qquad \text{uniform distance}$$

If we want to steer the beamforming in the θ direction, the phase-shift (Φ) between the antennas has to be :

$$\Phi = -2\pi\frac{d}{\lambda}\sin\theta_{max} \qquad \text{max radiation direction}$$

The distance between the antennas, d, is $\lambda/2$. It satisfies the grating lobes condition for every number of antennas. This fixed value is not the optimal value for a specific number of antennas in a certain direction. The optimal equation can be found with the following equations [38].

$$\psi^{\text{visible}} \in [-kd + \Phi; kd + \Phi]$$
$$2\pi\frac{d}{\lambda} + \Phi \leq 2\pi - \frac{2\pi}{N} \qquad \text{end of visible range at last zero}$$
$$\frac{d}{\lambda} \leq (1 - \frac{1}{N}) - \frac{|\Phi|}{2\pi}$$
$$\frac{d}{\lambda} \leq \frac{1}{1+\sin(\theta)}(1 - \frac{1}{N})$$

Adapting the $\frac{d}{\lambda}$ can also be done to have a thinner beam-steering increasing the spatial multiplexing overall. Taking the biggest $\frac{d}{\lambda}$ respecting this condition leads to the thinnest beamwidth without grating lobes.

Due to the Beamforming, the signal of the multiple TX antennas combines on the only receptor as follows :

$$r = \underbrace{\begin{bmatrix} h_1 & ... & h_{N_{TX}} \end{bmatrix}}_{\text{Channel Matrix}} \underbrace{\begin{bmatrix} BF_{T,1} \\ ... \\ BF_{T,k} \\ BF_{T,N_{TX}} \end{bmatrix}}_{\text{BeamForming TX}} s + w$$

$$r = \begin{bmatrix} h_1 & ... & h_1 e^{(jN_{TX}\Delta\Phi)} \end{bmatrix} \begin{bmatrix} 1 \\ ... \\ e^{(-jN_{TX}\Delta\Phi)} \end{bmatrix} s + w$$

Where h_1 is the channel between the user and the antenna 1, $BF_{T,1}$ is the beamforming weight at the first antenna and s is the signal sent, w the noise and r the received signal.

All signals combine in phase due to the beamforming being done to correct the delay of the channel. And therefore, we can observe an antenna gain in this direction.

If multiple RX antennas are used for one stream.

$$r = \underbrace{\begin{bmatrix} BF_{R,1} & ... & BF_{R,N_{RX}} \end{bmatrix}}_{\text{BeamForming RX}} \begin{bmatrix} h_{1,1} & ... & h_{1,N_{TX}} \\ h_{2,1} & ... & ... \\ h_{N_{RX},1} & ... & h_{N_{RX},N_{TX}} \end{bmatrix} \begin{bmatrix} BF_{T,1} \\ ... \\ BF_{T,N_{TX}} \end{bmatrix} s + w$$

Where $BF_{R,1}$ is the beamforming weight of the first RX antenna, and $h_{1,1}$ is the channel between the first RX antenna and the first TX antenna.

We can multiply the 2 beamforming vectors and the channel matrices to have a virtual channel matrix between the streams and not the antennas anymore.

For multiple users with the same number of RX antennas $\frac{N_{RX}}{N_s}$, several beamforming at the receiver and at the transmitter are used.

$$\mathbf{r} = \underbrace{\begin{bmatrix} BF_{R,1,1} & \dots & BF_{R,1,N_{RX}} \\ BF_{R,N_s,1} & \dots & BF_{R,N_s,N_{RX}} \end{bmatrix}}_{\text{BeamForming RX}} \begin{bmatrix} h_{1,1} & \dots & h_{1,N_{TX}} \\ h_{2,1} & \dots & \dots \\ h_{N_{RX},1} & \dots & h_{N_{RX},N_{TX}} \end{bmatrix} \underbrace{\begin{bmatrix} BF_{T,1,1} & BF_{T,1,N_s} \\ \dots & \\ BF_{T,N_{TX},1} & BF_{T,N_{TX},N_s} \end{bmatrix}}_{\text{BeamForming TX}} \begin{bmatrix} s_1 \\ \dots \\ s_{N_s} \end{bmatrix} + w$$

$$= \underbrace{\begin{bmatrix} BF_{R,1,1} & \dots & 0 \\ 0 & \dots & BF_{R,N_s,N_{RX}} \end{bmatrix}}_{\text{BeamForming RX}} \begin{bmatrix} h_{1,1} & \dots & h_{1,N_{TX}} \\ h_{2,1} & \dots & \dots \\ h_{N_{RX},1} & \dots & h_{N_{RX},N_{TX}} \end{bmatrix} \underbrace{\begin{bmatrix} BF_{T,1} & 0 \\ \dots & \dots \\ 0 & BF_{T,N_{TX},N_s} \end{bmatrix}}_{\text{BeamForming TX}} \begin{bmatrix} s_1 \\ \dots \\ s_{N_s} \end{bmatrix} + w$$

Where $BF_{R,N_s,N_{RX}}$ is the beamforming weight of the last antenna of the last user and s_1 is the signal from the first user and $\mathbf{r}$ is the received vector of signals of every user.

The Beamforming matrices are diagonal by blocks because the analog beamforming is done per stream. On the receiver side, the signal could not come from the other antennas than the one from its beamforming so that part is not changeable (users are not connected). On the transmitter side, it is done in the same way where each stream is associated with 1 beamforming array. This design could be different and Figure 3.6 illustrates the 2 types of hybrid beamforming. In this work, we are using a sub-connected Hybrid beamforming instead of a fully connected one. The sub-connected consumes less power than the fully connected, but the latter provides more gain in spectral efficiency.

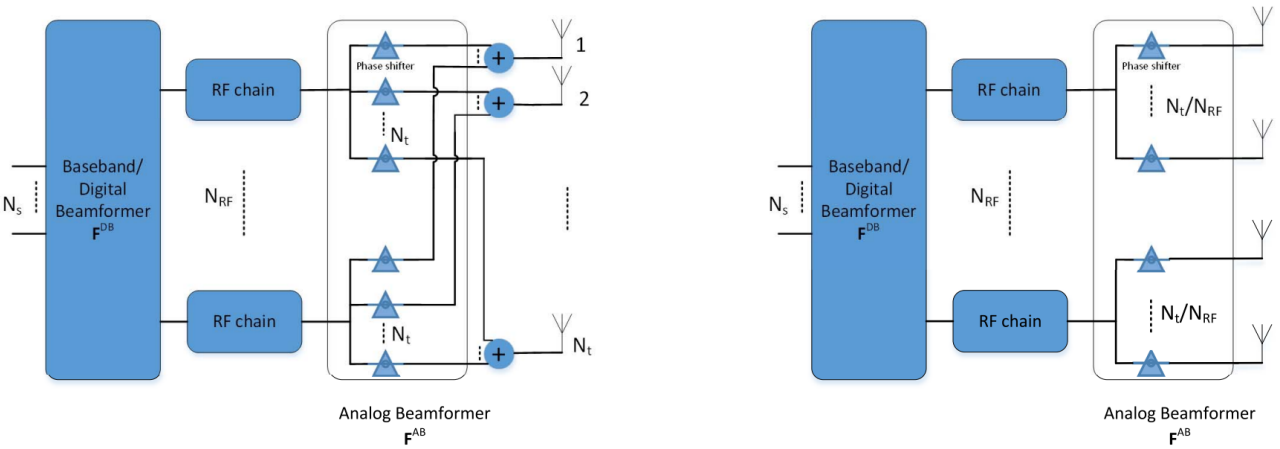

a. Fully connected hybrid beamforming

b. Sub-connected hybrid beamforming

Figure 3.6: The 2 types of Hybrid Beamforming [2]

The precoder is added before the beamforming at the transmission to increase the spatial efficiency and therefore, the performance.

$$\mathbf{r} = \underbrace{\begin{bmatrix} H_{V,1,1} & ... & H_{V,1,N_s} \\ H_{V,N_s,1} & ... & H_{V,N_s,N_s} \end{bmatrix}}_{\text{Virtual channel}} \underbrace{\begin{bmatrix} P_{1,1} & ... & P_{1,N_s} \\ P_{N_s,1} & ... & P_{N_s,N_s} \end{bmatrix}}_{\text{Precoder}} \begin{bmatrix} s_1 \\ ... \\ s_{N_s} \end{bmatrix} + w$$

By using a Zero-Forcing (ZF) precoder, if the estimation of the channel is perfect, the precoder will have this form: $P = H_V^{-1}$. The multiplication of the 2 will be the identity matrix. But if there is noise in the estimation, the performance of this precoder could drop. There is also the Maximum Combining Transmission (MCT). This precoder has this matrix: $P = H_V^H$. The MCT algorithm is based on multiplying the channel matrix by its hermitian matrix to get the maximum power in the diagonal. This type of precoder maximizes the power of the received signal in the dominant direction and mitigates the impact of interference. It is working a bit like analog beamforming for which the goal is to maximize the power on the diagonal, hence maximizing the SNR. If the two are used, the virtual channel matrix will be even more directed on the diagonal and diagonally dominant, making it look like an Identity matrix in the end.

ZF is aimed to completely eliminate the interference between the different streams, by arranging nulls in the direction of the other users. MCT precoder maximizes the SNR and the maximum mean square error (MMSE) precoder is a precoder that makes a trade-off between SNR maximization and interference mitigation. But its complexity is even bigger than the Zero-Forcing hence, increasing the power computation. It was not analyzed in this work.

4 SIMULATIONS RESULTS

4.1 Setup

In this chapter, the SISO and the MU-MIMO communications are analyzed.

For a reminder, Orthogonal Frequency Division Multiplexing (OFDM) is the digital modulation scheme used for the simulation with quadrature amplitude modulation (QAM). Most simulations will be done with the LoS component only, meaning a Rician channel with only one path. This hypothesis can be done for high frequency, as the other NLOS components are much degraded. In the simulations, synchronization is supposed to be perfect and thus only the data(no pilots) is sent.

The sampling frequency was fixed to 1GHz on the power model. It is linear with the power consumption and does not impact the simulations so it can be scaled easily.

Other parameters of the simulations are as follows, the size of the FFT is 512, the CP is 128, the number of taps(excluding the central tap) of the SRRC filter is 8 with a roll-off factor of 0.2, and the coherence BW is 15.

4.2 SISO simulations

To begin with, a synchronized communication was used with 16-QAM OFDM on a LoS channel with a code rate of 13/16 with an oversampling factor of 2 and a Square-Root Raised Cosine (SRRC) filter.

Each block was first analyzed to observe the effect of the quantization on one block only. The other blocks were using the quantization level of MATLAB. Hereunder is an example of the IFFT in figure 4.1. Each color represents a different quantization level. This figure shows that the performance of the simulation is good (with a

degradation of less than 0.5dB) until 4 quantization levels are used.

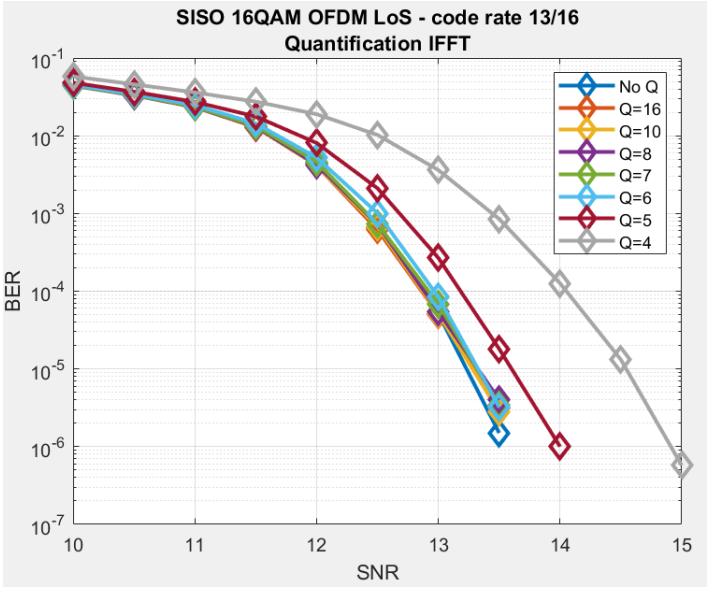

Figure 4.1: Quantization of the ifft

This was done for all the blocks separately. After that, the SNRs required to achieve a BER of 10^{-3}, 10^{-4}, and 10^{-5} for each simulation were recorded. They are putted in figure 4.3 with their power consumption associated.

For the coded version with code rate=13/16 and on the Rician channel with a LoS component exclusively, we get the results in Figure 4.3. All the points represent the scenarios regarding the power of the digital part only of the communication chain with respect to the SNR to achieve a certain BER. The color with the legend "Constant" means that the simulation was done with the quantification level the same for all the communication blocks. The color for ifft, pulse shaping,... are related to the simulations where only these algorithms were quantized. No difference in the BER performance between the quantization level of 16 and the quantization from MATLAB was observed. Therefore, for the power consumption of the blocks with the quantization level from MATLAB, the quantization level was assumed to be 16. And finally, the "Optimal" is a combination of quantization at several levels.

To find the possible optimal quantization levels, a heuristic process to perform simulations is done based on how to decrease the power consumption without increasing the SNRs. From the simulation with a constant quantization level, we produced the figure 4.2. In this figure, we can see the percentage of the power of

each block.

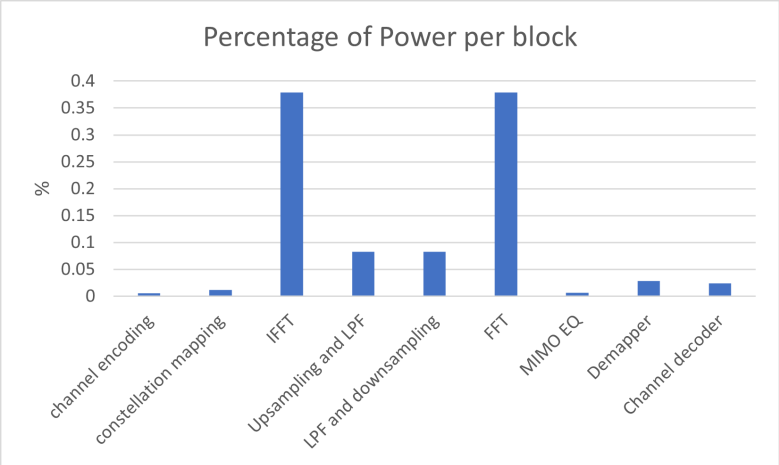

Figure 4.2: Power consumption of this SISO scenario with constant quantization

The blocks of FFT and IFFT consume the most power and their performance is still good for low quantization levels. The pulse shaping filter and the match filter do not consume as much and their performance decreases faster.

This is why the configurations tested are with all the blocks at a quantization level of 10 and the IFFT and/or the FFT at 7. Or the rest at a quantization level at 8 and the IFFT at 7. The different configurations can be seen in a table in Annex B.1.

The optimal quantization for this scenario depends on what is the optimization function. The cost function is related to the power to achieve a certain SNR and the power to decrease the energy of the communication by reducing the quantization. A possible optimal quantization would be to take Q=7 for the fft and the ifft and Q=10 for the rest. In this case, a power saving of 52.06% compared to the full 16-bit computation can be made and 17.83% compared to 10-bit.

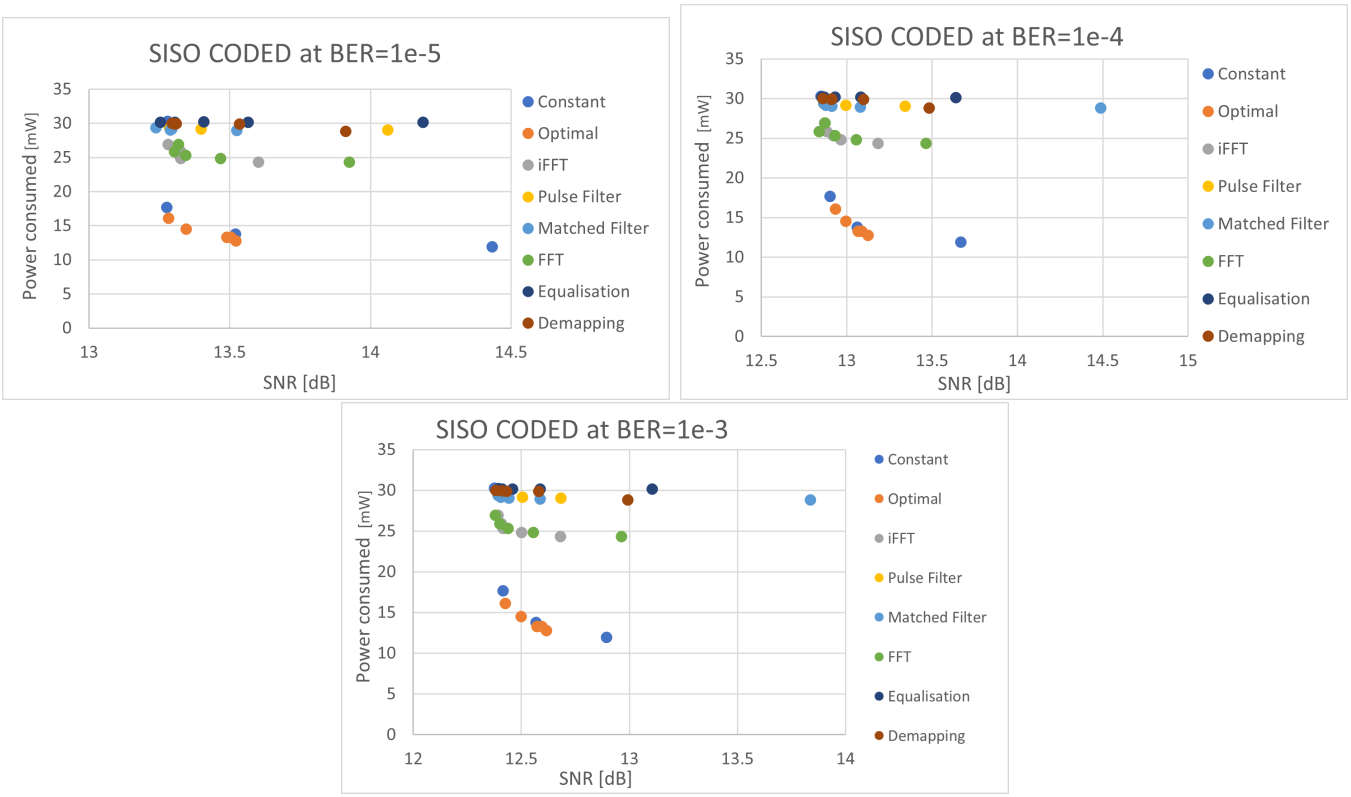

Figure 4.3: Power consumed of the digital chain with SNR to achieve this performance

Communications on different channels were also analyzed for SISO communication such as the Rician channel. We choose the same K-factor of the Rician fading channel as the one used in other research for mm-Wave frequencies [20]. It has a value of 13.3 dB and this corresponds to a normalized power in the LoS direction of $\frac{K}{1+K} = 95.5\%$. Another channel, with the power in the LoS direction of 50%, is also simulated to see the degradation in this case. The parameters of these channels are shown in the table 4.1.

LoS energy fraction	0.955 Or 0.5	fraction of the total energy for the LOS component = K/(1+K)
Delay limit	20	maximum delay spread in taps(not including LoS tap)
Density	0.2	Probability to have a tap at any position between 1 and the max delay spread
Decay	4	factor by which the average NLOS tap energy decays over the maximum delay spread

Table 4.1: Rician Fading Channel Parameters

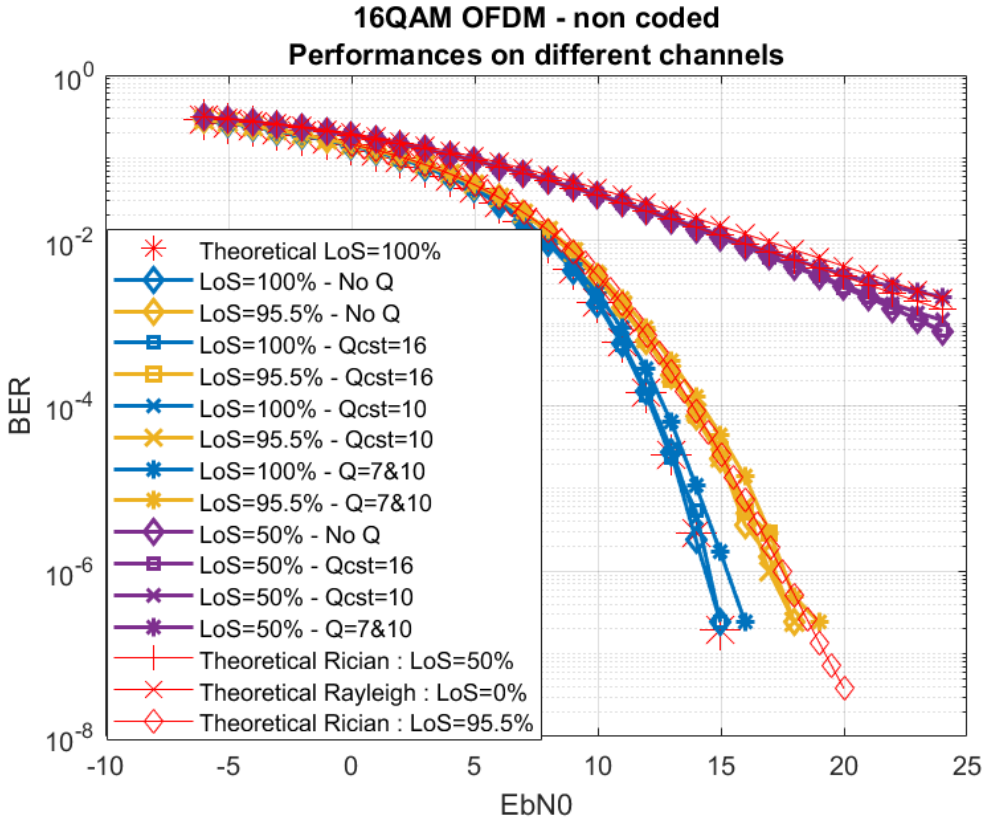

Figure 4.4: Quantization impact on channel degradation

Figure 4.4 illustrates the performance of the quantization on 3 different channels. The one with only the LoS component reaches the theoretical limit of the 16-QAM constellation. The other channel, the Rician fading channel, never reaches this theoretical LoS limit and has a shift in Eb/N0 of approximately 2dB at a BER of

10^{-5}. The quantization for both has the same impact on the performance. The optimum can therefore be found for the same level of quantization when operating on this Rician fading channel.

For the third type of channel, half the power was sent in the LoS direction. The performance till Q=10 for all blocks were approximately the same as the ones without quantization. And they reach the theoretical limit of this Rician channel. But the optimal version has not in this case the same behaviour as for the previous model.

We can also observe that the Rayleigh has almost the same curve as the Rician with 0.5. It is because if the LoS direction has not the majority of the power, it could also be considered as one path of the Rayleigh fading channel.

Then the effect of the SRRC filter was analyzed. Figure 4.5 shows the error metric for the filters. It is the sum of the energy of the convolution at all non-central samples. In Figure 4.5, the 2 parameters are the length of the filter (number of taps including both sides of the baseband filter without the center: T) and the roll-off factor (α). From this figure, we can choose which filter to use based on its performance.

	4	6	8	10	12	14	16	18	20
0.1	-15.69	-18.86	-21.77	-24.69	-27.82	-31.35	-35.54	-40.67	-45.74
0.15	-17.58	-22.10	-26.98	-32.99	-41.23	-44.78	-41.40	-40.61	-41.75
0.2	-19.89	-26.62	-35.96	-44.83	-39.74	-39.65	-42.80	-49.65	-53.23
0.25	-22.81	-33.73	-43.62	-38.20	-40.24	-47.87	-51.86	-47.20	-48.59
0.3	-26.64	-47.05	-37.42	-39.85	-51.42	-47.77	-46.77	-53.90	-56.22
0.35	-32.19	-38.61	-37.77	-49.64	-46.67	-46.95	-59.71	-51.87	-53.40
0.4	-42.93	-35.85	-42.72	-47.89	-45.89	-60.93	-50.68	-56.06	-58.07

Performance better than -15 -20 -25 -30 -40 (dB, sum energy at other sample positions for filter * filter)

Figure 4.5: Performance of the filter regarding the Roll-off factor and the filter length coming from internal research from IMEC

Simulations with 64-QAM non-coded bits are used because we can get more sensible results and see more effectively the impact of the filter parameters. The quantization was done on the pulse-shaping filter only.

We first analyze the effect of quantization with filters with approximately the same performance errors. For this, the filters taken were the filters with an error less than -40dB such as the one with ($\alpha : 0.1$,$T = 18$), ($\alpha : 0.2$,$T = 10$), and ($\alpha : 0.4$,$T = 4$) in figure 4.6.

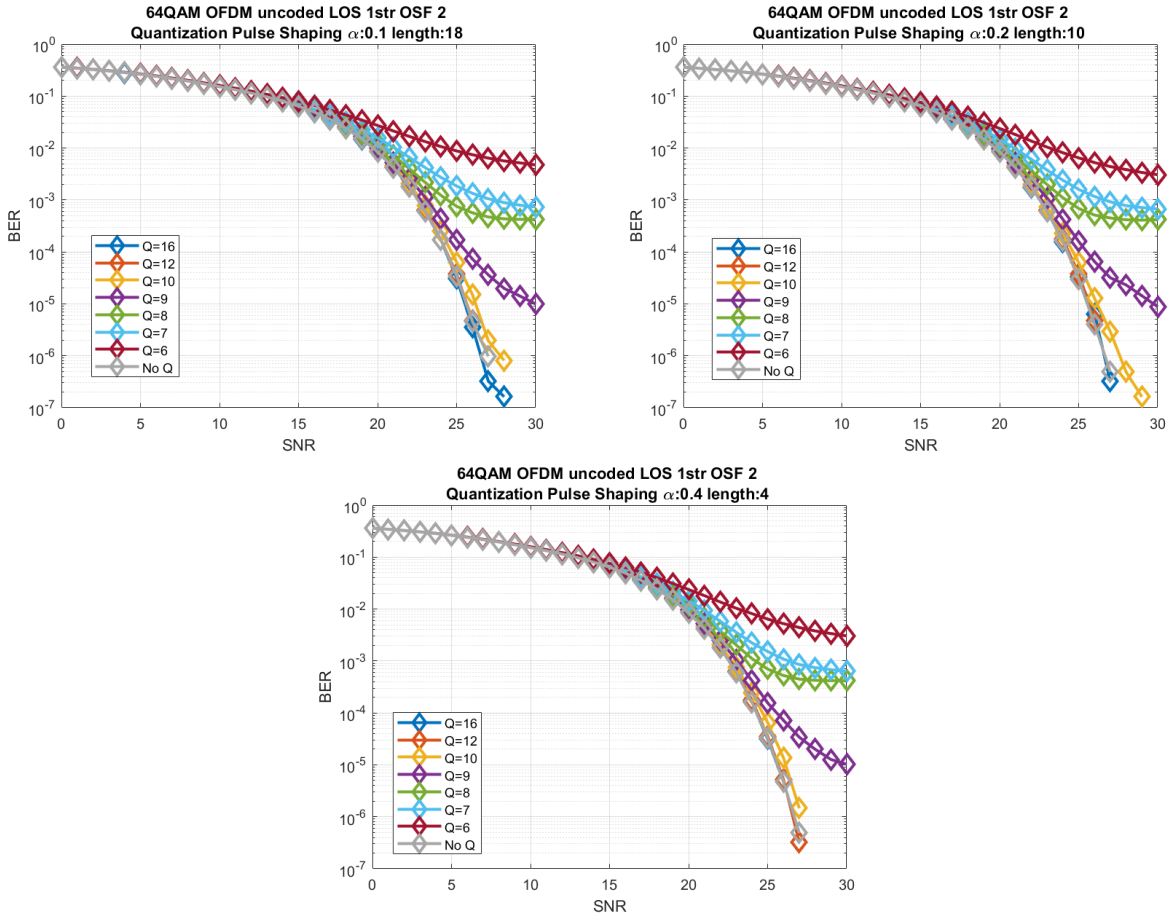

Figure 4.6: Performance Quantization with filters of same error from Figure 4.5

In Figure 4.6, we can observe no real difference in performance between the quantized simulations of the several filters. All the filters have the same performance and the quantization on a longer filter has not a bigger decrease in performance than the quantization over a smaller filter.

Then, the impact of quantization on the intrinsic performance of the filter was also studied. For this, the filters used all have the same roll-off factor of 0.1 but different lengths.

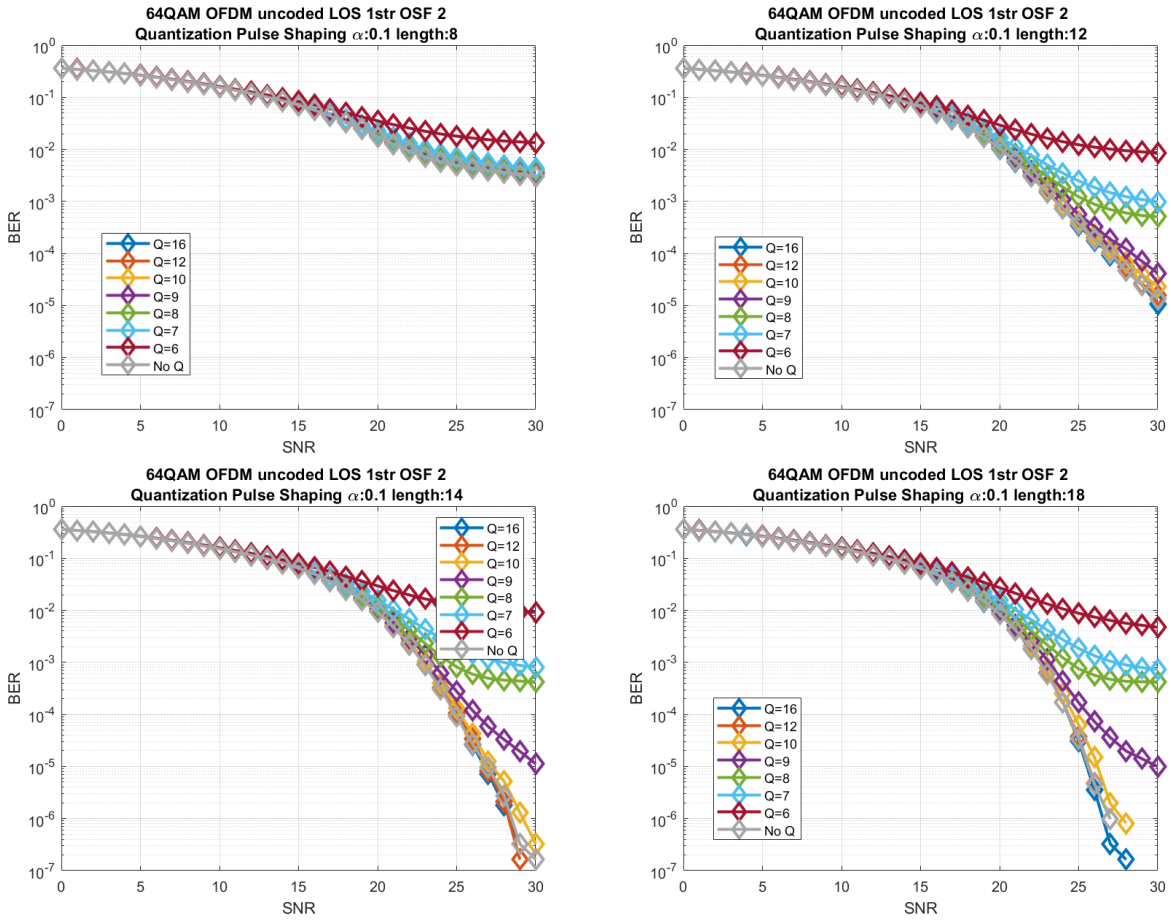

Figure 4.7: Performance Quantization with filters of different error from Figure 4.5

Figure 4.7 illustrate that first, if the intrinsic performance of the filter is worse than the -25dB, the BER does not achieve 10^{-4} and hardly 10^{-3}. Then it also shows that the loss of the filter with no quantization does not affect the performance of the low-quantization simulations unless the losses are bigger than the ones from the quantization.

In conclusion, the filter has to have good performance (-30/-40dB) to have a working communication. Then the quantization has no combined effect with the filter's performance. If the filter has a bad performance, then we should use a smaller quantization level to reduce the power consumption.

4.3 MIMO simulation

The configuration used is only one antenna at each receptor. The angle of arrival is thus always 0. We also suppose that the array of antennas at TX is on the same horizontal line. The users are all further away so the elevation angle between the users is approximately the same. Its impact is limited therefore it is not considered and only the azimuth angle θ is.

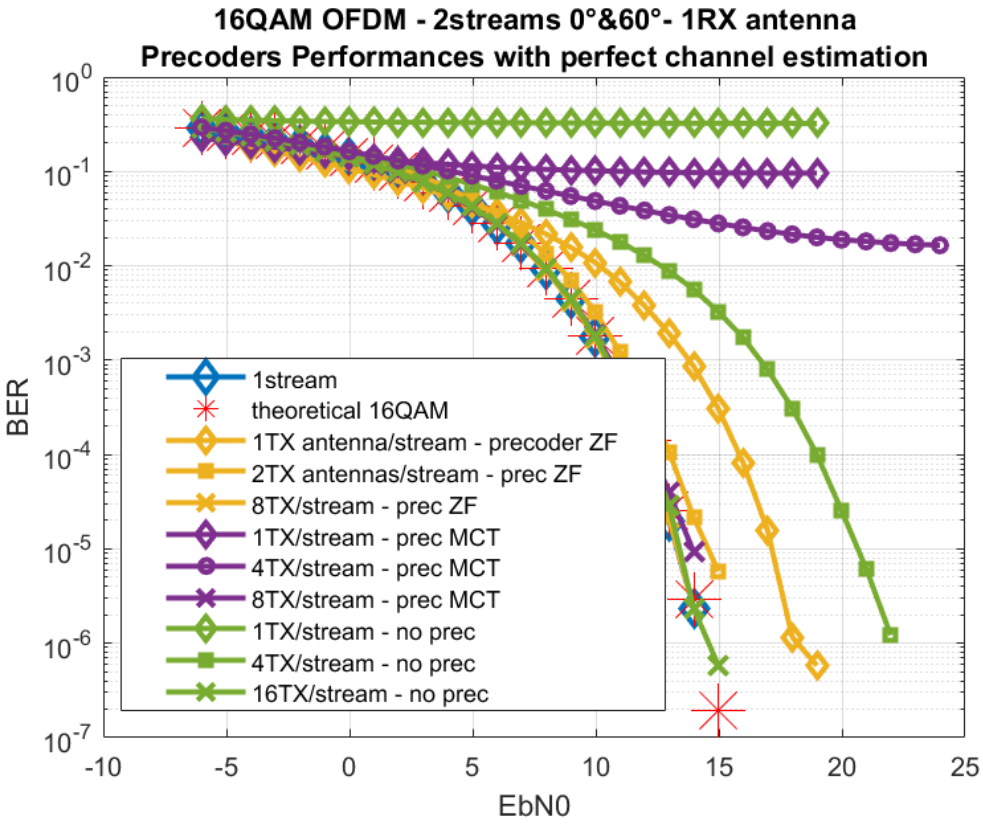

Figure 4.8: Precoder Performance

In figure 4.8, we can see several precoding techniques, the ZF precoding, the MCT precoding, and no precoder which is analog beamforming only. Figure 4.8 shows that for 1 antenna per user, the MCT precoder cannot transmit the data efficiently as well as without a precoder. This comes because both signals come from isotropic antennas and the signal from both streams comes with the same power to the users. The channel matrix is not diagonally dominant so the power maximization is not efficient. With more antennas, the analog beamforming is better and so, the MCT precoder has better performance [7].

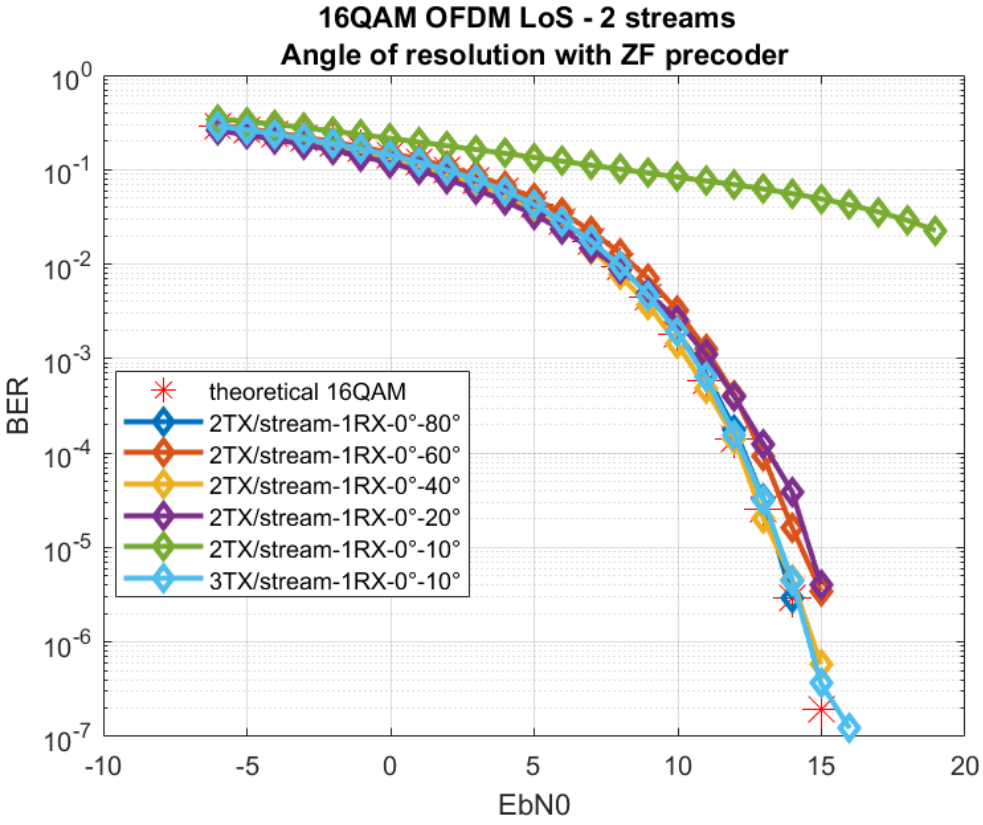

Figure 4.9: Angle of Resolution with a ZF precoder

In Figure 4.9, we can see the BER curves for several directions of the users. The BER reaches the theoretical curve with 2 antennas until the users are 10° apart or with 3 antennas for this case. Figure 4.9 shows that even with a perfect ZF precoder, the data cannot be transmitted correctly if the users are too aligned with each other. In this case, more antennas at TX are needed to have a better beam-steering. And if the distinction between the 2 users can be made, the performance become good again. The spatial separation of the beams cannot be done for 4 antennas and interference cannot be corrected by the ZF precoder. The channel matrix is not well conditioned in the case of 2TX antennas with 10° of difference between the users. It has a condition number of 11.13dB while it has a value of 6.84dB with 3 antennas. The channels with less than 10dB are suitable for spatial multiplexing [33].

If there is enough spatial separation between the transmit and receive antennas (regarding the condition number), it is possible to use multiple signal paths/streams(N_s).

This allows to increase the channel capacity(C) given by this formula [39]:

$$C = N_s B \log_2(1 + SNR) \tag{4.1}$$

Where B is the channel Bandwidth.

Then the effect of the different constellation sizes is also analyzed.

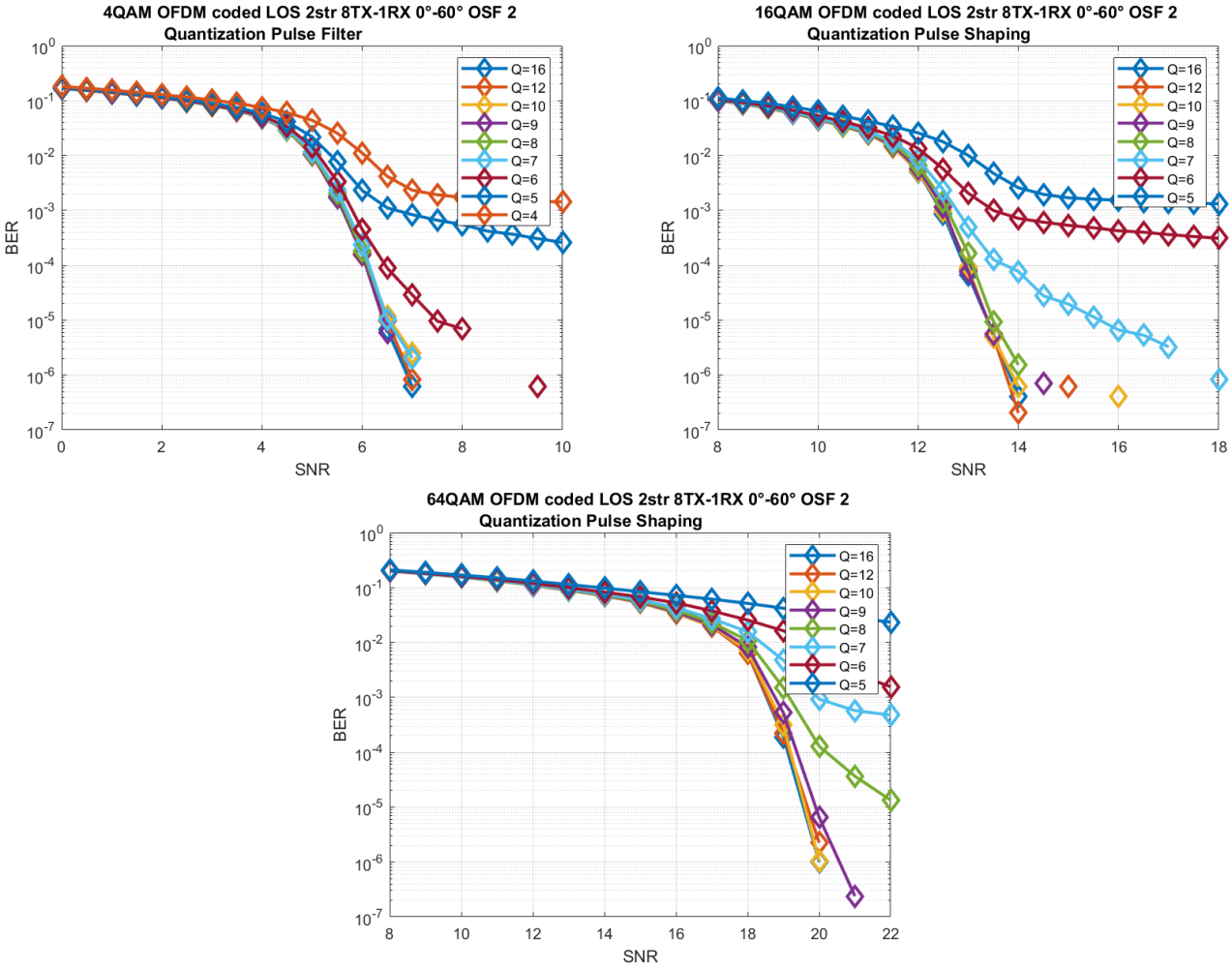

Figure 4.10: Performance of the M-QAM

In Figure 4.10, we see the BER curves for the 4-QAM, 16-QAM, and 64-QAM for several quantization levels of the pulse-shaping filter. Figure 4.10 shows that for the increasing constellations, one quantization level bigger is needed to have the same behavior. It increases at the same rate as the symbols. From 4-QAM to

16-QAM, the symbols are represented with 2 more bits, one in each direction and so is the quantization number for the blocks.

As the number of users for these simulations was small(2 streams for most simulations), the complexity of the precoder was not a big contributing factor in terms of power consumption. And because there is no estimation of the channel performed in the simulation, the effect of a small preamble or long preamble cannot be seen.

The performance is globally the same as for SISO communication. The simulations were done with 16-QAM OFDM LoS with an LDPC code rate of 13/16 on 2 streams in the directions of 0° and 60°. We construct Figure 4.11 in the same way as for Figure 4.3 in SISO communication.

Figure 4.11: Power consumed of the digital chain with SNR to achieve this performance

Figure 4.11 illustrates that the behavior for the MU-MIMO is globally the same as the SISO system. It has a factor of a bit more than 2 for 2 streams because of the precoding operations. To find the optimal case in this system, we use the same idea as for the SISO system. The IFFT and the FFT consume the most and the distortion of the pulse shaping filter is bigger in the MIMO system. The quantization level of the filter is the limiting factor so it is kept bigger. In this case, an optimal quantization is $Q = 10$ for the pulse shaping filter and the matched filter and $Q = 8$ for the rest. A table taking all the points of the optimal MIMO is kept in Appendix B.2.

The power saving between a full digital block on 16-bit and the optimized version with a 0.15dB of loss at a BER of 10^{-5} is 52.93%. The saving between a full digital on 10 bits and the optimized one is 19.75%. And for Tb/s communications, this represents a lot (250W for TX and RX) [10].

At 1.76GHz, for 4.165Mbps, the power consumption of the digital baseband computation is in between 20%-40% with an overall quantization level of 10. And it would be more around the 40% for terabits communication [10].

5 CONCLUSION

This thesis aimed to refine the digital processing part of the power model from IMEC by improving the way to characterize the different types of operations. For this, the algorithms of the communications were analyzed more thoroughly in terms of all the types of operations.

Then the second part was to analyze the effect of the quantization on the simulation of several scenarios in SISO and MU-MIMO. With this, a graph on the trade-off between related SNR and the power of the digital baseband computation has been made. This graph contains several configurations of quantization for each block and then an optimal configuration for the scenarios was chosen.

According to this model, around 20% of power savings can be made compared to a full 10-bits digital computation, reducing the power consumption.

Unfortunately, the power consumption of the paper which gives an energy consumption per type of operation does not give the same range of power consumption from the paper of the previous model.

The previous model from IMEC supposes 150 Giga operations per second per Watt for 4-bit complex arithmetic operations on a 40nm technology[10]. For the other assumptions related to the type of operation, we have the values from Figure 2.3. We assume that there is the same number of complex additions and multiplications so it corresponds to a mean number of 2 real additions and 2 real multiplications. If we want to see if they correspond we can do the following computation :

$$\begin{aligned} 2(0.032 \times 4) + 2(0.032 \times 4^2) \quad [pJ] &\stackrel{?}{=} \frac{1}{150 \times 10^9} \quad [J] \\ 0.36 \quad [pJ] &\stackrel{?}{=} 6.67 \quad [pJ] \end{aligned}$$

The factor of difference between the 2 formulas is 18.4. The difference between

them is significant so, other papers will need to be analyzed to see which constant to use for the different operations.

Additionally, a hypothesis was taken that access to SRAM was necessary to store the data in between the blocks. Using only registers might be possible in the design too. This would decrease a lot the power consumption as this operation is 50 times more consuming and therefore the optimization would need to be redone.

For a typical mm-Wave channel, the energy fraction of the LoS component is around 95.5% and the optimization configurations done on a fully LoS channel are still true.

We can also conclude that concerning the filter, only its intrinsic performance influence the BER and the performance of the filters are not correlated to the quantization. Therefore, the trade-off between roll-off related to the bandwidth and length of the filter length is still valid.

And concerning the constellation size, the optimal quantization configuration can be adapted by changing the quantization accordingly to the number of bits to represent the symbols. For example, for 64-QAM, the quantization level will be using 1 bit more in I/Q components compared to 16-QAM.

Several improvements can be added for future research. To have a more robust simulation model, taking the carrier frequency offset (CFO), the sampling clock offset (SCO), the IQ imbalance, and the phase noise could be done in the simulation. The packet would need to include the preamble and pilots.

Furthermore, the quantization steps could be done after each basic operation inside of the "black boxes" of the blocks (such as the fft A,...) to have a more realistic simulation.

Moreover, in the plot of the SNR and the power of the chain, the SNR could also be expressed in terms of the power of the chain to see what is the optimal point between quantization savings and transmission power. This way, we could analyze, for example, what is the power consumption of the PA needed to get the same performance as if no quantization was done. Do the quantization losses compensate for the increase of SNR for the same performance?

Then the peak-to-average power ratio (PAPR) is a problem for OFDM. Sending signals on multiple subcarriers creates sometimes constructive interference between them which results in high peaks while the average amplitude is low. This has effects on the quantization because it can on one side create saturation or on the other side low resolution. It can also add some distortions to the PA (saturation of

the PA). A block reducing it at emission after upsampling and before the PA could be added to the block diagram [6].

In a simulation with packets containing pilots, another type of equalizer could be analyzed. For now, only linear equalizers were used for their low consumption and simplicity. The non-linear equalizer like the Maximum Likelihood (ML) equalizer or the sphere decoding (SD) could be analyzed [27].

BIBLIOGRAPHY

[1] Samir Ahmad. *Quantifying the energy cost savings from 2G/3G network shutdowns*. 2022. URL: https://www.mtn-c.com/quantifying-the-energy-cost-savings-from-2g-3g-network-shutdowns/.

[2] Irfan Ahmed et al. "A Survey on Hybrid Beamforming Techniques in 5G: Architecture and System Model Perspectives". In: *IEEE Communications Surveys & Tutorials* 20.4 (2018), pp. 3060–3097. DOI: 10.1109/COMST.2018.2843719.

[3] Ray Andraka. "A survey of CORDIC algorithms for FPGA based computers". In: *Proceedings of the 1998 ACM/SIGDA sixth international symposium on Field programmable gate arrays*. 1998, pp. 191–200.

[4] Gunther Auer et al. "How much energy is needed to run a wireless network?" In: *IEEE wireless communications* 18.5 (2011), pp. 40–49.

[5] Subhankar Bhattacharjee et al. "Simulation, design and analysis of a low power MIMO-OFDM system and its implementation on FPGA". In: *2011 International Conference on Recent Trends in Information Systems*. 2011, pp. 88–93. DOI: 10.1109/ReTIS.2011.6146846.

[6] Sandrine Boumard et al. "Power consumption trade-off between power amplifier OBO, DPD, and clipping and filtering". In: *2014 26th International Teletraffic Congress (ITC)*. 2014, pp. 1–5. DOI: 10.1109/ITC.2014.6932968.

[7] Qasim Chaudhari. *Maximum Ratio Transmission (MRT)*. Nov. 24, 2021. URL: https://wirelesspi.com/maximum-ratio-transmission-mrt/.

[8] P. Danziger. *9.8 Complexity*. 2005. URL: https://math.ryerson.ca/~danziger/professor/MTH108/Handouts/gauss-complexity.pdf.

[9] Claude Desset. "Soft demappers: simple implementations". Nov. 2009.

[10] Claude Desset et al. "A flexible power model for mm-wave and THz high-throughput communication systems". In: *2020 IEEE 31st Annual International Symposium on Personal, Indoor and Mobile Radio Communications*. 2020, pp. 1–6. DOI: 10.1109/PIMRC48278.2020.9217264.

[11] Arinjoy Dutt et al. “Error-Correcting Codes in 5G and Beyond”. In: *International Journal of Engineering Research* 10.7 ().

[12] André Bourdoux François Horlin. *Digital Compensation for Analog Front-Ends: A New Approach to Wireless Transceiver Design*. Wiley, 2008.

[13] *Fujitsu developed the world's most efficient J-band power amplifier for 6G high-speed communications : Fujitsu Global*. en. URL: https://www.fujitsu.com/global/about/research/article/202302-inp-mos-hemt.html (visited on 07/24/2023).

[14] Marco Giordani et al. “Toward 6G Networks: Use Cases and Technologies”. In: *IEEE Communications Magazine* 58.3 (2020), pp. 55–61. DOI: 10.1109/MCOM.001.1900411.

[15] Sarah L. Harris and David Money Harris. “Digital Design and Computer Architecture ARM® Edition”. In: Elsevier, 2016. Chap. 5.2 Arithmetic Circuits.

[16] Alaa Hassan et al. “Evaluation of Complexity Versus Performance for Turbo Code and LDPC Under Different Code Rates”. In: Jan. 2012.

[17] F. Horlin et al. “Low-Complexity EM-based Joint CFO and IQ imbalance Acquisition”. In: *2007 IEEE International Conference on Communications*. 2007, pp. 2871–2876. DOI: 10.1109/ICC.2007.477.

[18] Mark Horowitz. “1.1 Computing's energy problem (and what we can do about it)”. In: *2014 IEEE International Solid-State Circuits Conference Digest of Technical Papers (ISSCC)*. 2014, pp. 10–14. DOI: 10.1109/ISSCC.2014.6757323.

[19] Sven Jacobsson et al. “Linear Precoding With Low-Resolution DACs for Massive MU-MIMO-OFDM Downlink”. In: *IEEE Transactions on Wireless Communications* 18.3 (2019), pp. 1595–1609. DOI: 10.1109/TWC.2019.2894120.

[20] Daisuke Kosuge and Hiroyuki Otsuka. “Transmission Performance of OFDM-based 1024-QAM under Different Types of Multipath Fading Channels”. In: *2021 IEEE VTS 17th Asia Pacific Wireless Communications Symposium (APWCS)*. 2021, pp. 1–5. DOI: 10.1109/APWCS50173.2021.9548774.

[21] F.R. Kschischang, B.J. Frey, and H.-A. Loeliger. “Factor graphs and the sum-product algorithm”. In: *IEEE Transactions on Information Theory* 47.2 (2001), pp. 498–519. DOI: 10.1109/18.910572.

[22] *Lecture Notes LELEC2796 : Multi-Antenna Channels and Systems*. 2017.

[23] Meng Li et al. “High-Speed LDPC Decoders Towards 1 Tb/s”. In: *IEEE Transactions on Circuits and Systems I: Regular Papers* 68.5 (2021), pp. 2224–2233. DOI: 10.1109/TCSI.2021.3060880.

[24] Ye Li. “Simplified channel estimation for OFDM systems with multiple transmit antennas”. In: *IEEE Transactions on Wireless Communications* 1.1 (2002), pp. 67–75. DOI: 10.1109/7693.975446.

[25] Yinsheng Liu et al. “Channel Estimation for OFDM”. In: *IEEE Communications Surveys & Tutorials* 16.4 (2014), pp. 1891–1908. DOI: 10.1109/COMST.2014.2320074.

[26] Robert Mailloux. *Phased Array Antenna Handbook, Third Edition*. 2017.

[27] Bernardo Martinez Blas. “Channel estimation and equalization in multiGigabit systems”. B.S. thesis. Universitat Politècnica de Catalunya, 2011.

[28] Amirhossein Mohammadian and Chintha Tellambura. “RF Impairments in Wireless Transceivers: Phase Noise, CFO, and IQ Imbalance – A Survey”. In: *IEEE Access* 9 (2021), pp. 111718–111791. DOI: 10.1109/ACCESS.2021.3101845.

[29] P.H. Moose. “A technique for orthogonal frequency division multiplexing frequency offset correction”. In: *IEEE Transactions on Communications* 42.10 (1994), pp. 2908–2914. DOI: 10.1109/26.328961.

[30] *Phased Array Antenna Patterns—Part 1: Linear Array Beam Characteristics and Array Factor | Analog Devices*. URL: https://www.analog.com/en/analog-dialogue/articles/phased-array-antenna-patterns-part1.html (visited on 06/21/2023).

[31] J.G. Proakis and D.G. Manolakis. “8.1 Efficient Computation of the DFT: FFT Algorithms”. In: *Digital Signal Processing*. Pearson custom library. Pearson, 2013. ISBN: 9781292025735. URL: https://books.google.be/books?id=ZoISngEACAAJ.

[32] Yinan Qi, Mythri Hunukumbure, and Yue Wang. “Millimeter wave los coverage enhancements with coordinated high-rise access points”. In: *2017 IEEE Wireless Communications and Networking Conference (WCNC)*. IEEE. 2017, pp. 1–6.

[33] Stefan Schindler and Heinz Mellein. “Assessing a MIMO channel”. In: *Rohde & Schwarz white paper, Tech. Rep* (2011).

[34] Peter August Simonsen and JT Kristensen. “Power Consumption in DFTs for OFDM Systems”. PhD thesis. Master Thesis, Institute for Electronic Systems, Aalborg University, Denmark . . .

[35] Harsh Tataria et al. “6G wireless systems: Vision, requirements, challenges, insights, and opportunities”. In: *Proceedings of the IEEE* 109.7 (2021), pp. 1166–1199.

[36] Zongjie Tu and Shiyong Zhang. “Overview of LDPC Codes”. In: *7th IEEE International Conference on Computer and Information Technology (CIT 2007)*. 2007, pp. 469–474. DOI: 10.1109/CIT.2007.7.

[37] Luc Vandendorpe. *Slides LELEC2795 : Orthogonal frequency division multiplexing: OFDM*. 2021.

[38] Giusseppe Vecchi. *Slides Array Antennas: Linear (1D) Arrays*. 2022.

[39] Lochan Verma, Mohammad Fakharzadeh, and Sunghyun Choi. “Wifi on steroids: 802.11AC and 802.11AD”. In: *IEEE Wireless Communications* 20.6 (2013), pp. 30–35. DOI: 10.1109/MWC.2013.6704471.

[40] Lifang Wang. *Implementation of Low-Density Parity-Check codes for 5G NR shared channels*. 2021.

[41] Hen-Geul Yeh and Victor R Ramirez. “Implementation and Performance of a M-ary PSK and QAM-OFDM System in a TMS320VC5416 Digital Signal Processor”. In: *2007 Second International Conference on Digital Telecommunications (ICDT'07)*. IEEE. 2007, pp. 19–19.

[42] Chu Yu et al. “A low-power 64-point pipeline FFT/IFFT processor for OFDM applications”. In: *IEEE Transactions on Consumer Electronics* 57.1 (2011), pp. 40–40. DOI: 10.1109/TCE.2011.5735479.

APPENDIX

A ALGORITHM FFT

Algorithm of the FFT with radix 2 written in Python. The quantization steps could be added in this code in future simulations.

```
def fft_opcount(a,countadd,countmult):
    """
    Recursive algorithm performing the Fast Fourier Transform
    and returning also the number of operations
    acc : vector containing the the Fourier Transform
    countadd : the number of complex additions
    countmult : the number of complex multiplications
    """
    N = len(a)
    if (N<=1):
        return a,countadd,countmult
    a_even,countadd_even,countmult_even = fft_opcount(a[::2],countadd,countmult)
    a_odd,countadd_odd,countmult_odd  = fft_opcount(a[1::2],countadd,countmult)

    countadd = countadd_even+countadd_odd
    countmult=countmult_even+countmult_odd
    acc = 1j*np.zeros(N)

    for i in range(N//2):
        m = np.exp(-2j*np.pi*i/N)*a_odd[i]
        countmult += 1
        acc[i]      = a_even[i]+ m
        acc[i+N//2] = a_even[i]- m
        countadd  += 2
    return acc,countadd,countmult
```

B OPTIMAL CONFIGURATIONS

B.1 SISO

Power	BER=1E-05	BER=1E-04	BER=1E-03	Configuration
16.09	13.282	12.933	12.425	Q=7 for ifft , rest Q=10
14.52	13.344	12.996	12.498	Q=7 for fft/ifft , rest Q=10
13.28	13.490	13.088	12.595	Q=7 for fft, rest Q=8
13.28	13.504	13.067	12.571	Q=7 for ifft, rest Q=8
12.76	13.522	13.124	12.615	Q=7 for fft/ifft, rest Q=8

B.2 MU-MIMO

Power	BER=1E-05	BER=1E-04	BER=1E-03	Configuration
44.86	13.397	12.941	12.353	Q=7 for ifft , rest Q=10
41.71	13.516	13.003	12.398	Q=7 for fft/ifft , rest Q=10
37.78	13.342	12.878	12.363	Q=10 pulse/match, rest=8
34.54	13.818	13.313	12.694	Q=10 pulse/match, rest=7

UNIVERSITÉ CATHOLIQUE DE LOUVAIN
École polytechnique de Louvain
Rue Archimède, 1 bte L6.11.01, 1348 Louvain-la-Neuve, Belgique | **www.uclouvain.be/epl**